JPRS L/8800

5 December 1979

USSR Report

PHYSICS AND MATHEMATICS

(FOUO 5/79)

Quantum Electronics

FBIS FOREIGN BROADCAST INFORMATION SERVICE

NOTE

JPRS publications contain information primarily from foreign newspapers, periodicals and books, but also from news agency transmissions and broadcasts. Materials from foreign-language sources are translated; those from English-language sources are transcribed or reprinted, with the original phrasing and other characteristics retained.

Headlines, editorial reports, and material enclosed in brackets [] are supplied by JPRS. Processing indicators such as [Text] or [Excerpt] in the first line of each item, or following the last line of a brief, indicate how the original information was processed. Where no processing indicator is given, the information was summarized or extracted.

Unfamiliar names rendered phonetically or transliterated are enclosed in parentheses. Words or names preceded by a question mark and enclosed in parentheses were not clear in the original but have been supplied as appropriate in context. Other unattributed parenthetical notes within the body of an item originate with the source. Times within items are as given by source.

The contents of this publication in no way represent the policies, views or attitudes of the U.S. Government.

For further information on report content call (703) 351-2938 (economic); 3468 (political, sociological, military); 2726 (life sciences); 2725 (physical sciences).

APPROVED FOR RELEASE: 2007/02/08: CIA-RDP82-00850R000200030010-5

JPRS L/8800

5 December 1979

USSR REPORT

PHYSICS AND MATHEMATICS

(FOUO 5/79)

QUANTUM ELECTRONICS

Moscow KVANTOVAYA ELEKTRONIKA in Russian Vol 6, No 9, Sep 79
pp 1866-1870, 1903-1910, 1932-1941, 1953-1959, 1966-1970,
2024-2027, 2033-2034, 2036-2038

CONTENTS PAGE

LASERS AND MASERS

CONTENTS (Continued) Page

LASERS AND MASERS

UDC 678:539.26

DECISIVE ROLE OF VISCOELASTIC PROPERTIES OF POLYMERS IN THE MECHANISM OF THEIR LASER DESTRUCTION

Moscow KVANTOVAYA ELEKTRONIKA in Russian Vol 6 No 9, Sep 79 pp 1866-1870
manuscript received 16 Apr 79

[Article by M.I. Aldoshin, B.G. Gerasimov, A.A. Manenkov and V.S. Nechitaylo, Scientific Research Institute of Organic Intermediate Products and Dyes, Moscow, USSR Academy of Sciences Physics Institute imeni P.N. Lebedev, Moscow]

[Text] A study is made of the laser destruction of organic glasses with the repeated and onetime effect of radiation pulses of nanosecond duration. A correlation is established between the laser strength of transparent polymers and their viscoelastic properties, in particular, their yield point.

Investigations made earlier [1] have shown that an important role in the mechanism of the laser destruction of polymers with the effect on them of nanosecond radiation pulses is played by the viscoelastic properties of the matrix. In recent times studies [2-4] have appeared in which the laser strength of organic glasses is explained by their tendency toward carbonization during thermolysis [2] or by their supermolecular structure [3]. In [4] a molecular method is suggested for regulating the laser strength of polymethyl methacrylate (PMMA). However, the conclusions of the authors of [2-4] were made without taking into account the viscoelastic properties of polymers and in the absence of control of their optical purity (from the viewpoint of the presence and dimensions of absorbing inclusions).

This study has been made for the purpose of further studying the mechanism of the laser destruction of transparent polymers and the relationship between the laser strength of these polymers and their viscoelastic properties.

For the purpose of eliminating the influence of the optical purity of polymers on the results of investigation of their laser strength, in the experiments were used the same materials, the optical purity of which remained unchanged, and whose viscoelastic properties were varied by adding to the polymer a highly volatile plasticizer or by changing the temperature of the specimens over a wide range (from -60 to +80°C).

A determination was made of the bulk failure threshold of polymers with a single burst, I_d , under the influence of a giant (length of approximately 20 ns) radiation pulse of a ruby laser focused by a lens with a focal length of $f = 4$ cm , as well as of their laser strength with the repeated effect of radiation pulses of a fixed prethreshold strength, I_f , determined by the number of laser bursts, N , prior to the appearance in the matrix of macroscopic (approximately greater than 100 μ) fractures.

In one series of experiments with specimens of PMMA, the initial content of highly volatile plasticizer in which equaled 20 percent, a determination was made of I_d and N from the degree of volatilization of the plasticizer. It is obvious from fig 1 that with a decrease in concentration of the plasticizer and with an increase because of this in the yield point, σ_{ve} , of the polymer, I_d and N are reduced. A similar reduction in the laser strength of plasticized PMMA (with a fixed plasticizer content of 20 percent) is observed also with lowering of its temperature: With $T = +20°C$, $N > 10^4$, and with $T = -60°C$, $N \approx 10^3$.

In another series of experiments an investigation was made of the laser strength of unplasticized PMMA at different stages of polymerization (fig 2). As in [1,3], with an increase in conversion of the monomer, the sample's I_d is diminished. A rise in its temperature results in an increase in I_d , which is apparently associated with a reduction in σ_{ve} in heating. With an increase in conversion of the monomer N is also reduced (for a monomer $N > 10^4$ and for PMMA $N \approx 20$).

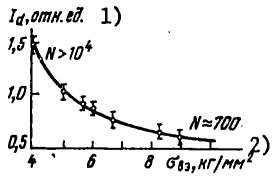

Figure 1. Reduction in Laser Strength Under the Onetime and Repeated Effect of Radiation Pulses in Proportion to Volatilization of the Plasticizer and an Increase in the Polymer's Yield Point

Key:
1. I_d , relative units
2. σ_{ve} , kg/mm^2

An increase in the optical purity of the monomer results in even more drastic reduction in the failure threshold in the process of conversion of the monomer into a polymer (table). Let us note that the effect of a reduction of I_d in the process of conversion from the state of liquid aggregation to the solid state is apparently of a general nature, which has been confirmed by us in freezing organic solvents (e.g., glycerine).

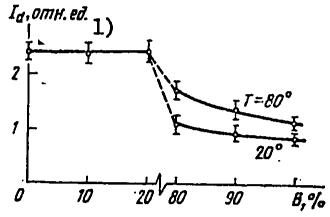

Figure 2. Dependence of Bulk Failure Threshold, I_d, on Degree of Conversion of the Monomer, B

Key:

1. I_d, relative units

Table

	3) Исходный		4) Очищенный		6) ПММА с пластификатором (20%)
	ММА	5) ПММА	ММА	ПММА	
$\sigma_{хр}$, кг/мм² 1)		8*)		8*)	
$\sigma_{пэ}$, кг/мм² 2)		12		12	3,9
I_d	2,4	1,0	70	3,5	1,4
N		20		90	$>10^4$

7) *) Справочные данные

Key:

1. σ_{khr} [brittle failure], kg/mm²
2. σ_{ye} [yield point], kg/mm²
3. Initial
4. Purified
5. PMMA
6. PMMA with plasticizer (20 percent)
7. Handbook data

Experimental investigations have shown that with the repeated effect of laser radiation with a strength of $I_f < I_d$ thoroughly purified PMMA withstands about 90 radiation pulses prior to the formation of macrofailure, whereas unpurified PMMA with the same strength, I_f, withstands about 20 radiation pulses (cf. table). Such an insignificant (from 20 to 90 radiation pulses) increase in the laser strength of PMMA on account of improvement of its optical purity is practically the limiting increase for matrices whose yield point is higher than their brittle failure point. On the other hand,

plasticized PMMA withstands more than 10^4 radiation pulses of strength I_f even with a lower failure threshold.

These results demonstrate that for polymers with different viscoelastic properties there is no correlation between I_d and N. Consequently, a high value of I_d per se, obtained only on account of improvement of the optical purity of a polymer, cannot ensure a high value of N. For polymers with identical viscoelastic properties the correlation between N and I_d is observed fairly distinctly. It is obvious from fig 3 that with a 10-fold reduction in I_f relative to I_d unplasticized PMMA withstands not more than 100 radiation pulses, whereas plasticized PMMA withstands more than 10^4 laser bursts with a considerably lower (threefold) reduction in I_f relative to I_d (samples were selected with an identical failure threshold).

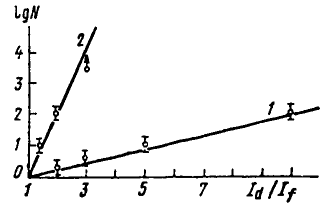

Figure 3. Laser Strength of Unplasticized (1) and Plasticized (2) PMMA with Onetime Effect of Radiation Pulses of Prethreshold Strength

For the purpose of revealing the nature of viscoelastic properties of polymers playing an important role in the mechanism of their laser destruction, by means of a plane polaroscope a study was made of the morphology of fractures in PMMA with the onetime effect of laser radiation of strength $I \lesssim I_d$. It was shown that in a series of successive laser bursts in the case of unplasticized PMMA a macrofracture measuring approximately greater than 100 μ arises in a threshold manner in the last burst of the series and is accompanied by a bright spark. Furthermore, around the fracture a stressed-state region is practically not observed. In plasticized PMMA after a certain number of bursts (the more, the greater the difference of $I_d - I_f$) a macrofracture originates, measuring approximately less than 10 μ, in the form of an opaque melted area gradually increasing in size with successive exposures. Furthermore, a visible glow is not observed, and the stressed-state area around the strain fracture is increased (fig 4a). In the last burst is observed a bright spark, a macrocrack is formed and almost total removal of stresses around the fracture takes place (fig 4b).

Figure 4. Photographs of Laser Micro- (a) and Macrofractures (b) in Plasticized PMMA with a Plane Polaroscope

Thus, in the laser fracturing of polymers a visually observed glow (spark) arises only in the process of formation of macrocracks and this is apparently caused by tribo-effects [5] accompanying failure of the material near absorbing flaws resulting from thermoelastic stresses.

Heating of unplasticized and plasticized PMMA to the vitrification temperature resulted in the total removal of stresses and strains around fractures, which testifies to their forced elastic nature. In this connection the correlation which we discovered between the laser strength of polymers and their yield point becomes understandable.

For the purpose of explaining the experimental results presented let us make use of the mechanism suggested in [1] for the laser fracturing of polymers, associated with their viscoelastic properties. As follows from an analysis of the system of heat conduction and elasticity equations, in a medium with an absorbing flaw important for the process of laser fracturing is parameter β, characterizing the thermoelastic properties of the matrix and equal to the ratio of the energy of strains in the medium caused by heating of the flaw to the energy of the laser radiation absorbed by it:

$$\beta = \frac{T_0}{C_V}\left(\frac{1+\nu}{1-\nu}\right)^2 \alpha^2 c_l^2, \tag{1}$$

where c_l is the velocity of sound, C_V is the specific heat, ν and α are the Poisson bracket and coefficient of linear thermal expansion, respectively, and T_0 is the initial temperature of the specimen. Substituting in (1) the parameters of PMMA gives $\beta = 0.06$, which exceeds by a few orders of magnitude β calculated by (1) for inorganic glasses (e.g., for fused quartz $\beta \sim 10^{-5}$). Consequently, the effectiveness of the conversion of the energy of laser radiation absorbed by a flaw into the energy of elastic strains of the matrix differs substantially for such "soft" materials as polymeric glasses, for which $\beta \gtrsim 10^{-2}$, and for such "hard" materials as fused quartz, sapphire and the like for which $\beta \lesssim 10^{-3}$. This difference results in the fact that in real (i.e., those containing absorbing flaws)

transparent dielectrics with $\beta \lesssim 10^{-3}$ laser fracturing originates as the result of the thermal rupturing of absorbing flaws [5-7], whereas in polymers ($\beta \gtrsim 10^{-2}$) elastic stresses comparable with breaking points originate with slight heating of the flaw.

Calculation of rupture stresses, $\sigma_{\theta\theta}$, near an absorbing flaw measuring $a > (\chi\tau)^{1/2}$ (χ is the thermal conductivity of the medium and τ is the length of the laser pulse) gives

$$\sigma_{\theta\theta}(t) = \beta \frac{C_V \rho}{3\alpha} \frac{T(t)}{T_0}, \tag{2}$$

where

$$T(t) = \frac{1}{C_V \rho (1+\beta)} \int_0^t Q(t')\, dt' \tag{3}$$

is the temperature of the absorbing flaw at moment of time t with a power density of the absorbed energy of Q; and ρ is the density of the medium.

Estimates made in accordance with (2) and (3) demonstrate that in PMMA $\sigma_{\theta\theta}$ stresses exceeding its breaking point are reached when the absorbing flaw is heated a total of 100°C. Therefore for the formation and development of a fracture in polymeric materials heating of flaws to considerable temperatures (when nonlinear effects of the absorption of the energy of laser radiation become substantial) is not necessary. In connection with this fractures are observed in polymers with considerably lower (by more than an order of magnitude) radiation strength as compared with the threshold strength for "hard" materials.

The experimentally observed dependence of the laser strength of polymers on their viscoelastic properties, as well as the correlation established between I_d and N and the yield point, can be explained in the following manner. It is a well-known fact that in the plasticization of polymers, as well as in heating them, the yield point, σ_{ve}, is reduced [8]. This results in the fact that in the process of pulsed heating of the absorbing flaw and a gradual increase in $\sigma_{\theta\theta}$ according to (2) the yield point is reached earlier than the breaking point. As a result, the material around the flaw experiences forced elastic strains characterized by considerable percentage elongation and is strain hardened severalfold as compared with the brittleness point, σ_{khr} [8]. In unplasticized PMMA the yield point is higher than the breaking point and the material is fractured in an embrittlement manner with the formation of cracks. The relationships given for σ_{ve} and σ_{khr} explain well the increase in the laser strength of plasticized PMMA with the onetime and repeated effect of radiation pulses as compared with unplasticized PMMA.

From this viewpoint the effect of a reduction in laser strength in the process of conversion from a monomer to a polymer also becomes understandable. The

fact is that in the conversion of a monomer we have PMMA plasticized by its own monomer. The reduction of the content of unpolymerized monomer results in an increase in the yield point and as a result in a corresponding reduction in laser strength.

The ideas developed here regarding the mechanism for the laser fracturing of polymers can be enlisted also for the purpose of explaining the increased strength of their surface as compared with their volume [9]. This fact is evidently associated with the difference in thermoelastic stresses originating in the vicinity of absorbing flaws located near the surface and in the material's bulk.

In conclusion the authors express their thanks to A.S. Bebchuk for his helpful discussion of the results of this paper and to V.A. Golovina for assistance in conducting the experiments.

Bibliography

1. Aldoshin, M.I., Gerasimov, B.G., Mizin, V.M. and Nechitaylo, V.S. "Tezisy VIII Vsesoyuz. konf. po kogerentnoy i nelineynoy optike" [Theses of the Eighth All-Union Conference on Coherent and Nonlinear Optics], Tbilisi, Metsniyereba, 1976, Vol 1, pp 136-137.

2. Butenin, A.V. and Kogan, B.Ya. KVANTOVAYA ELEKTRONIKA, 3, 1136 (1976).

3. Agranat, M.B., Novikov, N.P., Perminov, V.P. and Yampol'skiy, P.A. KVANTOVAYA ELEKTRONIKA, 3, 2280 (1976).

4. Yemel'yanov, G.M., Ivanova, T.F., Votinov, M.P., Ovchinikov, V.M., Piterkin, B.D. and Smirnova, Z.A. PIS'MA V ZHTF, 3, 687 (1977).

5. Danileyko, Yu.K., Manenkov, A.A. and Nechitaylo, V.S. KVANTOVAYA ELEKTRONIKA, 5, 194 (1978).

6. Danileyko, Yu.K., Manenkov, A.A., Nechitaylo, V.S. and Ritus, A.I. KVANTOVAYA ELEKTRONIKA, 1, 1812 (1974).

7. Danileyko, Yu.K., Manenkov, A.A. and Nechitaylo, V.S. ZHETF, 63, 1030 (1972).

8. Kargin, V.A. and Slonimskiy, G.L. "Kratkiye ocherki po fiziko-khimii polimerov" [Brief Synopses on the Physical Chemistry of Polymers], Moscow, Khimiya, 1967.

9. Bebchuk, A.S., Gromov, D.A. and Nechitaylo, V.S. KVANTOVAYA ELEKTRONIKA, 3, 1814 (1976).

CSO: 1862
8831

LASERS AND MASERS

UDC 621.375.826:537.523.5

GAS DYNAMICAL LASER WITH THERMALLY NONEQUILIBRIUM ELECTRIC ARC HEATING OF THE WORKING MEDIUM

Moscow KVANTOVAYA ELEKTRONIKA in Russian Vol 6 No 9, Sep 79 pp 1903-1910
manuscript received 24 Nov 78

[Article by B.V. Abakumov, Yu.V. Kurochkin, A.V. Pustogarov, N.N. Smagin, B.A. Tikhonov and V.V. Ukolov]

[Text] The feasibility is discussed of creating a gas dynamical laser (GDL) with thermally nonequilibrium electric arc heating of the energy carrying component of the working medium and with selective excitation of the optically active component by mixing it with the hot gas in the area of the critical cross section of the throat channel. The results are given of experimental investigations on detection of the vibrational nonequilibrium of nitrogen when it is heated in a high-current elevated-pressure arc discharge stabilized by rapid injection of the gas through the porous wall of the discharge channel. In the range of parameters realized in the experiment (I = 100 to 300 A, $p = (1 \text{ to } 2) \cdot 10^5$ Pa) the vibrational temperature of the ground state of nitrogen molecules exceeded the translational temperature of the gas by 1000 to 3000°K. An indication is given of the possible advantages of a GDL with thermally nonequilibrium electric arc heating as compared with a traditional GDL with equilibrium heating of the working medium.

1. Introduction

Interest in GDL's as sources of directed electromagnetic radiation for different technical applications has been growing steadily; however, characteristic of this type of laser are a number of disadvantages which considerably restrict their introduction in industry. First among these are the low efficiency of the conversion of thermal energy into laser radiation (0.5 to 2 percent) and the existence of expansion of the gas at high Mach numbers (M = 4 to 5). The first disadvantage results in the need to heat and pump a great mass of gas for the purpose of achieving high output power, and the second in complication of systems for delivering the working medium and exhausting the spent gas into the atmosphere.

Of course, the efficiency of the conversion of the thermal energy of the gas flow into induced emission for a GDL is determined by the competition

of two factors: by the level of vibrational energy stored in the gas, characterized by the vibrational temperature, T_v, and by the rate of DT relaxation, determined by the temperature of translational degrees of freedom, T_p. With thermodynamic equilibrium heating the maximum value of T_d is determined by the temperature of the gas in the inlet of the throat unit. For ordinary GDL's (heating of a preprepared mixture or production of it in the process of burning fuel) the optimal value of the braking temperature, T_0 = 1600 to 1800°K, is limited by collision relaxation losses in expansion of the gas in the throat unit [1].

The employment of GDL's with mixing of the optically active component (CO_2) with a preheated energy carrying component (N_2) has made it possible to raise the braking temperature of nitrogen to 2500 to 5000°K and to obtain experimentally record values of unit power output of 25 to 30 kJ/kg [2,3]. The most effective devices for heating gas to such high temperatures are electric arc high-pressure plasmatrons, which have been used successfully by a number of investigators for the purpose of heating gaseous working media in GDL's [3-5].

It must be mentioned, however, that in spite of the encouraging results obtained in model experiments the creation of steady-state GDL's with high-temperature heating and selective excitation of the working medium involves considerable difficulties. In this paper is considered the feasibility of improving the efficiency of a GDL with electric arc heating of the working medium by utilizing the effects of thermochemical nonequilibrium in the discharge, stabilized by the rapid transverse injection of gas through the porous wall of the channel. As experimental investigations have demonstrated, in an arc discharge of this type it is possible to heat the energy carrying component of the working medium, e.g., nitrogen, with the gas's vibrational temperature higher than its translational. Subsequent expansion of the nitrogen in the supersonic throat unit with mixing of the optically active component in the near-critical region of the throat, as the result of the high value of $T_v > 2000$°K, makes it possible to increase the inversion density, and the possibility of thereby lowering the translational temperature, $T_p <$ < 1500°K, permits expansion of the flow to lower Mach numbers of $M_p < 3$, which simplifies solving the problem of mixing components and exhausting the spent gas into the atmosphere.

2. Experimental Setup and Investigation Procedure

In an investigation of electric arc plasmatrons with delivery of the working medium through the porous wall of the discharge channel [6,7] it was discovered that as the result of rapid thermal and hydrodynamic interaction of the radial gas stream with the current conducting nucleus of the discharge are formed two zones which differ drastically in their parameters: a high-temperature zone of flow of ionized gas with low density, and a peripheral region of flow with a temperature close to the temperature of the injected gas. These two zones are separated by a region of quite high temperature gradients, velocities and concentrations of components of the arc plasma. The sudden change in parameters resulting from the rapid removal of heat

into the gas surrounding the arc, diffusion and also the difference at medium energies in the light and heavy components of the plasma are responsible for the possibility of its deviation from thermodynamic equilibrium.

For the purpose of solving this problem it is necessary to establish the existence or absence of equilibrium between the vibrational and translational degrees of freedom of molecules of the plasma forming gas, e.g., nitrogen, since it is precisely vibrational excitation of nitrogen which determines the inverse population density of the upper laser level of the radiating molecule, e.g., CO_2. For this it is necessary to measure the vibrational temperature of molecules of nitrogen in the electronic ground state and the translational temperature of the gas. The absence of equality between these temperatures will indicate deviation from equilibrium with regard to vibrational-translational degrees of freedom.

The experimental unit (fig 1) was a direct-current electric arc plasmatron. The arc discharge, 1, was struck between a cathode, 2, and anode, 5, separated by an insert, 3, between electrodes, with a cylindrical discharge channel made of a porous ceramic material, 4, through whose walls was injected the plasma forming gas--nitrogen. In the experiment were measured the current and voltage of the arc, the rate of flow of the gas and the pressure in the channel. The arc's radiation spectrum was photographed with a KS-55 spectrograph, 8, through quartz windows 6 and 7 in the middle cross section of the channel. Investigations were made with the following discharge parameters: arc current and voltage, I = 50 to 500 A , U = 200 to 1300 V ; intensity of injection of gas through porous wall, m = 2 to 16 kg/(m^2·s) ; pressure in channel, (1 to 20)·$\cdot 10^5$ Pa . The inside diameter and length of the channel equaled 0.02 and 0.05 m, respectively.

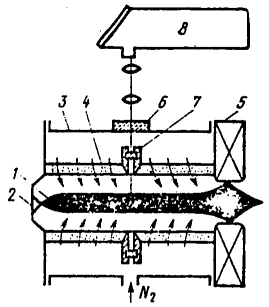

Figure 1. Sketch of Experimental Unit

The translational temperature of the gas was identified with the temperature of the population of rotational levels, which was determined from allowed rotational lines K = 12-56 of band 0-0 (391.4 nm) of the first negative system of nitrogen. The concentration of electrons, n_e , was determined from

the intensity of continuous radiation (λ = 495.5 nm), taking into account the contribution of the negative continuum [8].

Of course, direct measurement of the vibrational temperature of the ground state of a molecule of N_2, T_v ($X^1\Sigma_g^+$), requires the employment of special methods of IR diagnostics, the utilization of which under conditions of a high-current elevated-pressure discharge involves great difficulties and does not make it possible to analyze fully mechanisms for the origin of nonequilibrium. In this study, based on the results of [9], a method has been developed of determining T_v ($X^1\Sigma_g^+$) from the measured temperature of a molecular ion of nitrogen, N_2^+ ($B^2\Sigma_u^+$).

In [9] was established the absence of equilibrium between the electronic and atomic-ionic components of the plasma of a high-current arc discharge stabilized by the intense injection of nitrogen through the porous wall of the discharge channel. It was demonstrated that in a great portion of the channel's cross section the temperature for population and distribution of atoms by excited levels and the temperature of electrons substantially raise the translational temperature of the gas.

In another study by the same authors of [9] a determination was made of the composition of the nonequilibrium plasma of nitrogen and an analysis was made of the mechanisms for the population and deactivation of electron-excited levels of atoms, molecules and molecular ions, from which it follows that in the plasma of an elevated-pressure arc discharge a major role is played by collisions with heavy particles. State $B^3\Pi_g$ is excited in collision with vibrationally excited molecules and molecules in the metastable state $A^3\Sigma_u^+$. State $C^3\Pi_u$ is populated on account of step-by-step excitation by electron collision from state $B^3\Pi_g$. Consequently, under the conditions considered it is not possible to determine the vibrational temperature of the ground state of a molecule from vibrational temperatures of electronically excited states of molecules obtained by measuring the intensity of bands 1^+ and 2^+ of the positive system of nitrogen, as was done for low-pressure discharges [10].

It is another matter with the state of the molecular ion of nitrogen N_2^+ ($B^2\Sigma_u^+$), which is populated primarily by electron collision and is deactivated in the process of extinguishing with electrons. In one case and the other considerable disruption does not take place in the nature of distribution by vibrational energy levels, since the moment of momentum and the vibrational energy in population of $B^2\Sigma_u^+$ by electron collision vary but slightly, in addition to which the potential energy curve for N_2^+ ($B^2\Sigma_u^+$) is shifted but slightly in relation to the potential energy curve of the electronic ground state of nitrogen ion N_2^+ ($X^2\Sigma_g^+$), as a result of which the distributions by vibrational energy level in these states are similar. Consequently, the temperature, T_v ($B^2\Sigma_u^+$), measured in the experiment should agree with the vibrational temperature of the ground state of the ion, T_v ($X^2\Sigma_g^+$). Since the exchange of vibrational quanta between molecule N_2 and ion N_2^+ takes

place as the result of the rapid charge transfer reaction $N_2 + N_2^+ \rightarrow N_2^+ + N_2$ and the characteristic exchange time is two to three orders of magnitude shorter than the VT relaxation time [11], it is possible to state that $T_v (B^2\Sigma_u^+)$ equals $T_v (X^2\Sigma_g^+)$ equals $T_v (X^1\Sigma_g^+)$. The transfer of vibrational energy from N_2 to N_2^+ as the result of the charge transfer reaction, caused by the difference in the magnitude of the vibrational energy quantum of molecules ($\omega_{N_2} = 2359\ cm^{-1}$ and $\omega_{N_2^+} = 2207\ cm^{-1}$), does not result in a difference in vibrational temperatures of molecules N_2 and N_2^+, since this effect under the conditions considered will be substantial only at fairly low translational temperatures ($T_p < 1000°K$), e.g., under conditions of a low-pressure glow discharge.

In our experiment the vibrational temperatures of the different electronic states of molecules and molecular ions of nitrogen were determined from the radiation intensities of the appropriate system of molecular bands. The absolute intensity was determined from a trace obtained in processing a photograph of the spectrum with an MF-4 microphotometer. The sensitivity and its dependence on the wavelength were determined from the spectrum of an SI-10-300 standard tungsten lamp. The error in measuring the absolute intensity of radiation equaled 40 percent. The error in measuring relative intensity, compared with reference to the ratio of the heights of peaks of a band to its area, did not exceed 20 percent.

The vibrational temperatures of a specific electronic state were determined from the tangent of the angle of the slope of the direct dependence of $\ln (J_{v'v''}/q_{v'v''}\nu^4)$ on the energy of the vibrational level, E_v, (where $J_{v'v''}$ and ν are the intensity and frequency of the radiation at the v'-v" transition and $q_{v'v''}$ is the Franck-Condon transition factor). An approximation was made of this dependence by the method of least squares. The vibrational temperature of state $B^2\Sigma_u^+$, which was identified with $T_v (X^1\Sigma_g^+)$, was measured in relation to 0-0, 0-1, 1-1, 1-2 and 2-4 transitions of the first negative system of nitrogen with an error of not greater than 30 percent with $T_v = 10^4°K$. The vibrational temperature of states of $N_2 (C^3\Pi_u)$ were measured in relation to 0-5, 1-5, 2-5, 3-8 and 4-10 transitions of the second positive system of nitrogen with an error of not greater than 16 percent.

3. Experimental Results

In fig 2 are given graphs of the distribution over the radius of the discharge channel (r = 1 cm) of the vibrational temperature of the ground state of the molecule N_2 ($T_v (B^2\Sigma_u^+) = T_v (X^1\Sigma_g^+)$) (curve 1) and of the translational temperature of the gas (curve 2). As can be concluded from these graphs, in a great portion of the channel the vibrational temperature is greater than the translational, which testifies to deviation from equilibrium with regard to vibrational-translational degrees of freedom, especially in the peripheral zone of the discharge.

Mention should be made of the fact that in peripheral regions of the discharge (r > 7 mm) according to [9] in population of state $B^2\Sigma_u^+$ a considerable role begins to be played by interactions with solid particles and identification of vibrational temperatures of the electron excited ground state of the molecular ion of nitrogen and of the ground state of the molecule requires additional

refinement. Nevertheless, as follows from fig 2, obtained with discharge parameters lying within the range of certainty for experimental determination of the vibrational temperature of the ground state of molecule N_2, the vibrational temperature is greater than the translational temperature of the gas by 2200°K (T_v = 4200°K and T_p = -2000°K). Let us note that, according to the results of [9], the degree of deviation from equilibrium and, consequently, the separation of T_v from T_p, their absolute values and the dimensions of the zone of existence of nonequilibrium make possible regulation of variation in the intensity of injection and in the discharge current. So, with an increase in injection and a steady discharge current the separation of T_v from T_p grows on account of a reduction in temperature of the gas. With an increase in current and steady intensity of injection the central equilibrium region of discharge is expanded and the separation of temperatures in the peripheral region is maintained with higher absolute values of T_p and T_v.

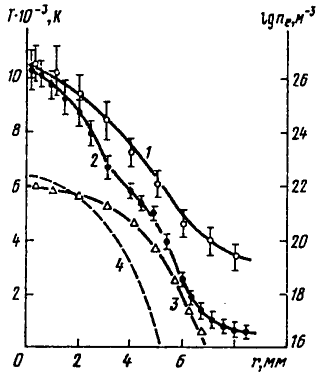

Figure 2. Experimental Distribution of Vibrational and Translational Temperatures and of Concentration of Electrons in Relation to Radius of the Channel

In fig 2 (curve 3) is given also the distribution, measured experimentally, of the concentration of electrons, n_e, as compared with that computed for an equilibrium composition in terms of temperature, $T = T_p$ (curve 4). From the results obtained it follows that deviation from equilibrium is expressed not only in a separation of temperatures, but also in concentrations of components of the plasma, e.g., electrons, considerably exceeding equilibrium values. For example, at r = 6 mm with T_p = 3000°K, $n_e = 10^{18}$ m^{-3}, whereas corresponding to the equilibrium case at the same temperature is $n_e = 5.4 \cdot 10^5$ m^{-3} [12].

Thus, the plasma of the arc discharge under the conditions discussed is not only nonequilibrium thermally, but also chemically, and the electric arc

plasmatron with stabilization of the discharge by means of intense "pore" injection in this case can be regarded as a generator of a stream of a nonequilibrium plasma of an elevated-density molecular gas.

4. Discussion of Results

The results obtained indicate the feasibility of utilizing vibrational nonequilibrium electric arc heating of the gas for the purpose of improving the efficiency of a GDL with excitation of the optically active component by mixing it with the heated gas. By combining the discharge chamber of the plasmatron with the receiver of the GDL's throat unit it is possible to arrange for removal of the gas into the throat from the nonequilibrium peripheral zone of a discharge with a moderate translational (T_p < 2000°K) and a high vibrational (T_v > 2000°K) temperature. Here it is important that the distance from this zone to the throat's critical cross section, where the vibrational energy is quenched, be less than the length of vibrational relaxation of nitrogen with the parameters of the gas in the receiver. Since the vibrational relaxation time for pure nitrogen at not too high a translational temperature (T_p < < 2000°K) is comparatively long, these conditions can be fulfilled. For example, with T_p = 1500°K and T_v = 4000°K (cf. fig 2), τ_{N_2} = 0.94 ms [11]. Assuming that the pressure in the receiver equals $p_0 = 10^6$ Pa, and the mean rate of flow in the subcritical section of the throat equals approximately 300 m/s, we get a relaxation length of ℓ_r = 28 mm, which testifies to the feasibility of withdrawing nitrogen into the throat while maintaining nonequilibrium vibrational excitation. A basic system for implementing one of the possible variants of such a unit is shown in fig 3.

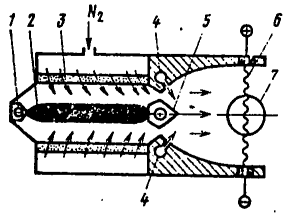

Figure 3. Diagram of GDL with Nonequilibrium Electric Arc Heating of the Working Medium: 1--cathode; 2--arc; 3--porous channel; 4--CO_2-He injection receiver; 5--anode; 6--glow discharge; 7--optical cavity

The advantages of nonequilibrium heating of the energy carrying component of the working medium is illustrated quantitatively in fig 4 for a CO_2-N_2 GDL. Illustrated in this figure is the supersonic throat of a GDL through which the nitrogen heated in the electric arc discharge is expanded with subsequent mixing in the near-critical section of the throat of a CO_2-He mixture, and illustrated conventionally is the change in translational and vibrational temperatures of the gas.

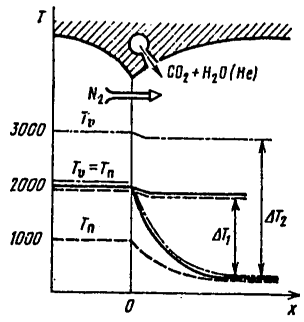

Figure 4. Qualitative Picture of Expansion of the Gas in the Supersonic Throat of the GDL

With equilibrium heating (solid-line curves) the inversion density is determined by the difference ΔT_1 (it is assumed that T_{N_2} (v = 1) equals T_{CO_2} (001) and T_{CO_2} (100) equals T_p . With nonequilibrium heating two variants are possible for increasing the efficiency of the GDL. In the first variant (dot-dash lines) even before the critical cross section of the throat $T_v > T_p$ and the inversion density is determined by the value $\Delta T_2 > T_1$, which generally corresponds to high energy output. The simplest quantitative estimate shows that with a value of $T_v - T_p = 2000°K$ before the throat's critical cross section the reserve of vibrational energy in the nitrogen which can be converted into induced radiation is three- to fivefold greater than in equilibrium heating of the nitrogen to $T_p = 2000°K$.

The advantages of the second variant of nonequilibrium heating (cf. fig 4, dotted lines) are evidenced in the fact that with a lowered translational temperature, T_p , for the purpose of achieving the same static parameters in the cavity are required lower Mach numbers, which simplifies the problem of mixing components, reduces losses on account of gas dynamical inhomogeneities in the stream and lowers the pressure in the throat unit's receiver required for exhausting the spent gas into the atmosphere through the supersonic exit cone.

Let us indicate two more advantages of nonequilibrium electric arc heating of the working medium of a GDL. The first consists in the ability to increase the pressure in the cavity, since the relaxation time, $\tau[CO_2(001)]$, is reduced linearly with an increase in pressure and is increased exponentially with a reduction in the gas's temperature. The second advantage consists in the fact that because of the reduction in the rate of collision deactivation of CO_2 molecules with lowering of T_p CO_2 in a mixture with H_2O or He can evidently be mixed in the subsonic zone of the throat unit, which considerably improves mixing efficiency and the homogeneity of the flow.

From the results of a determination of the composition of the nonequilibrium plasma of an arc discharge in [9] it follows that in the peripheral zone from which the gas is removed through the supersonic throat the concentration of electrons is considerably greater than the equilibrium ($n_e = 10^{17}$ to 10^{18} m^{-3}; cf. fig 2, curves 3 and 4). Taking into account the possibility of quenching the nonequilibrium concentration of electrons in the supersonic throat [13], in principle it is possible to introduce additional vibrational energy beyond the critical cross section of the throat, e.g., in the glow discharge [14]. In this case the main arc discharge in the plasmatron, in addition to heating the gas, will perform the role of a preionizer for the semi-self-maintained discharge in the region of the cavity (cf. fig 3).

5. Numerical Investigation

For the purpose of a quantitative verification of the influence of preliminary electric arc heating of nitrogen on characteristics of the inverse medium, a calculation was made of the supersonic flow of a vibrationally relaxing mixture of N_2-CO_2-He with a determination of inversion density and gain. Gas dynamics equations for the two-dimensional flow of a nonviscous and non-heat-conducting gas were solved by the method suggested in [15] together with equations for vibrational relaxation for a mixture of gases with four vibrational modes [16].

For the case of equilibrium heating, in the critical cross section of the throat was set a value of $T_p = T_v$, and for the purpose of modeling non-equilibrium heating, $\Delta T = T_p - T_v$. In modeling separate heating of the nitrogen and excitation of the optically active CO_2-He mixture was employed a model of instantaneous mixing. To the point of injection of the CO_2-He, the flow of the N_2-CO_2-He mixture was considered by taking into account only VT relaxation of N_2 for N_2. At the point of injection were included the mechanisms for the vibrational exchange of N_2 and CO_2, VV exchange in CO_2 and VT relaxation of CO_2 for N_2, CO_2 and He. Thus, the flows of N_2 and CO_2-He were separated (from the viewpoint of relaxation kinetics, but not of gas dynamics).

Calculations were made for a profiled throat with an expansion ratio of $A/A^* = 30$, a critical cross section height of 1 mm and a supersonic section height of 25 mm. The point of injection of the CO_2-He mixture, i.e., the point for including vibrational exchange of N_2 molecules with the optically active component, was set at coordinate x_v. Calculation with $x_v = 0$ can be regarded as modeling of simultaneous heating and expansion of the mixture. In fig 5 are given characteristic distributions over the axis of the throat of vibrational temperatures of nitrogen, T_4, of the antisymmetric mode of $CO_2(\nu_3)$, T_3, of the combined mode of $CO_2(\nu_1\nu_2)$, $T_2 = T_1$, of the translational temperature of the gas, T_p, of the absolute value of the inverse population, ΔN, and of the gain, α. It follows from this figure that for equilibrium and combined heating of the mixture ($x_v = 0$ and $\Delta T = 0$) the gain is $\alpha = 0.3$ m^{-1} (dotted line), which in order of magnitude agrees with the experimental results obtained under approximately the same conditions

[16]. Mixing the CO_2-He in the supercritical region at a distance of 4 mm downstream from the critical cross section with equilibrium heating (x_v = = 4 mm and $\Delta T = 0$) results in a fourfold increase in α (dot-dash line), which agrees qualitatively with the experiment in [1]. The results of modeling nonequilibrium heating ($\Delta T = 600°K$, $x_v = 4$ mm , solid-line curves in fig 5, and $\Delta T = 2500°K$, $x_v = 0$, fig 6) demonstrate the possibility of increasing the gain six- and 15-fold, respectively, as compared with equilibrium heating. Furthermore, the inversion density in the latter variant (cf. fig 6) equals $\Delta N = 3 \cdot 10^{17}$ cm^{-3} , which is an order of magnitude higher than the inversion value with ordinary high-temperature heating. The high value of the gain of $\alpha = 6$ m^{-1} with $\Delta T = 2500°K$ and $x_v = 0$ (cf. fig 6) is caused by the great difference in temperatures T_3 and T_2 , i.e., by the difference in populations of the upper and lower laser levels of CO_2 molecules. It is characteristic that in this case T_3 approaches T_4 more quickly than in the calculation variant in fig 5. This testifies to the effectiveness of the exchange N_2 (v = 1) + CO_2 (000) → N_2 (v = 0) + CO_2 (001) .

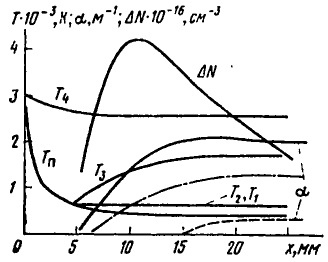

Figure 5. Calculated Distribution of Parameters Over Axis of Throat for Mixture 0.2 CO_2 + 0.35 N_2 + 0.45 He with $T_p = 2600°K$ and $p_0 = 1.8 \cdot 10^6$ Pa

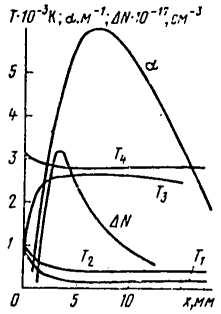

Figure 6. Calculated Distribution of Parameters Over Axis of Throat for Mixture of 0.1 CO_2 + 0.35 N_2 + 0.55 He with $T_p = 1000°K$, $\Delta T = 2500°K$ and $p_0 = 1.8 \cdot 10^6$ Pa and $x_v = 0$

Let us note in conclusion that the advantages of thermochemically nonequilibrium electric arc heating of the working medium of a GDL discussed in this article with a CO_2-N_2 GDL as an example can be more considerable when using as the energy carrying component gases such as CO or H_2, since the effectiveness of vibrational electron exchange in these gases is considerably greater than in nitrogen.

Bibliography

1. Kroshko, V.N., Soloukhin, R.I. and Fomin, N.A. FIZIKA GORENIYA I VZRYVA, 10, 473 (1974).

2. Krauklis, A.V., Kroshko, V.N., Soloukhin, R.I. and Fomin, N.A. FIZIKA GORENIYA I VZRYVA, 12, 792 (1976).

3. Tazan, I.P.E., Charpenel, M. and Borgki, R. "AIAA Paper, N73-622" (1973).

4. Shall, Migamoto, Horioka, Murasaki. JAP. J. APPL. PHYS., 15, N2 (1977).

5. Kasuma, Migamoto, Murasaki. JAP. J. APPL. PHYS., 15, N7 (1977).

6. Kurochkin, Yu.V. and Pustogarov, A.V. In "Eksperimental'nyye issledovaniya plazmatronov" [Experimental Investigation of Plasmatrons], Novosibirsk, Nauka, 1977 p 82.

7. Kurochkin, Yu.V., Pustogarov, A.V. and Ukolov, V.V. IZV. SO AN SSSR, SER. TEKH. NAUK, No 13, 23 (1978).

8. Biberman, L.M. and Norman, G.E. UFN, 91, 193 (1967).

9. Kurochkin, Yu.V., Polak, L.S., Pustogarov, A.V., Slovetskiy, D.I. and Ukolov, V.V. "Materialy VII Vsesoyuz. konf. po generatoram nizkotemperaturnoy plazmy" [Data of the Seventh All-Union Conference on Low-Temperature Plasma Generators], Alma-Ata, Kitap, 1977.

10. Novgorodtsev, M.Z., Ochkin, V.N. and Sobolev, N.N. Preprint FIAN, Moscow, 1969, No 172.

11. Yeletskiy, A.V., Palkina, L.A. and Smirnov, B.M. "Yavleniya perenosa v slaboionizovannoy plazma" [Transfer Phenomena in a Slightly Ionized Plasma], Moscow, Atomizdat, 1975.

12. Burchorn, F. and Wiencke, R. Z. PHYS. CHEM., 215, 265 (1960).

13. Bazhenova, T.V. and Lobastov, Yu.S. In "Svoystva gazov pri vysokikh temperaturakh" [Properties of Gases at High Temperatures], Moscow, Nauka, 1967.

14. Biryukov, A.S., Marchenko, V.M. and Shelepin, L.A. TRUDY FIAN, 83, 87 (1975).

15. Ivanov, M.Ya. and Krayko, A.N. ZHURN. VYCH. MAT. I MAT. FIZ., 12, No 3 (1972).

16. Losev, S.A., Makarov, V.N., Pavlov, V.A. and Shatalov, O.P. FIZIKA GORENIYA I VZRYVA, 9, 463 (1973).

CSO: 1862
8831

LASERS AND MASERS

UDC 621.378:535.3.087

QUANTUM STATISTICS OF THE PHOTOCURRENT OF OPTIMAL DETECTORS OF LIGHT RADIATION UNDER CONDITIONS OF ATMOSPHERIC 'VIEWING'

Moscow KVANTOVAYA ELEKTRONIKA in Russian Vol 6 No 9, Sep 79 pp 1932-1941
manuscript received 15 Jan 79

[Article by P.A. Bakut, K.N. Sviridov and N.D. Ustinov]

[Text] Taking into account quantum effects and registration noise, statistics were obtained and investigated, of the photocurrent of optimal detectors of incoherent broadband light radiation for different conditions of atmospheric "viewing." It has been demonstrated that the presence of atmospheric phase distortions results in alteration of the statistics for the photocurrent of optimal detection and worsens the energy characteristics of the distributions gotten.

Introduction

In recent years a number of studies have appeared, devoted to the optimal processing of coherent [1] and incoherent [2] light fields under conditions of atmospheric "viewing." Investigations conducted have demonstrated that optimal are those detectors which form quadratic functionals of the detected light field. However, in these studies the quantum effects of registration [2] are either totally not discussed or the influence of turbulence of the atmosphere on their statistics is not taken into account [1]. In connection with this, in this study is considered the influence of turbulence of the atmosphere on statistics of the photocurrent of optimal detectors of incoherent broadband light radiation.

1. Realization of Optimal Detection

Based on the investigations made in [2], the quadratic functional, Z , of detected incoherent broadband light radiation, $E(\rho,t)$, synthesized in the absence of atmospheric phase distortions, has the form

$$Z=\frac{1}{2}\frac{1}{(2\pi)^2}\int\limits_{-\infty}^{\infty}d\omega\int\limits_{S_0}V(\mathbf{r},\omega)\,d\mathbf{r}\left|\int\limits_{S_A}\int\limits_{0}^{T}E(\boldsymbol{\rho},t)\,e^{-i\omega t}H_{\omega}(\boldsymbol{\rho}-\mathbf{r})\,dt\,d\boldsymbol{\rho}\right|^2, \tag{1}$$

where

$$V(\mathbf{r}, \omega) = \frac{1}{N_0} \frac{J(\mathbf{r})/N_0}{1 + [J(\mathbf{r})/(2\pi N_0)]} J(\omega) = V(\mathbf{r})\, J(\omega); \tag{2}$$

$J(\mathbf{r})$ is the spatial distribution of the object's intensity; N_0 is the spectral power density of the background radiation; $J(\omega)$ is the frequency distribution of the object's intensity in the transmission band of the processing system; S_0 is the area of the object's projection onto the picture plane (the plane located near the object and perpendicular to its viewing line); $H_\omega(\rho - \mathbf{r})$ is a function characterizing in a Fresnel approximation the propagation of light waves from the picture plane of the object, $\mathbf{r}$, to the plane of the telescope's receiving aperture, ρ; and S_A is the area of the telescope's receiving aperture.

Taking (2) into account, expression (1) can be rewritten in the form

$$Z = \frac{1}{2} \frac{1}{(2\pi)^2} \int_{S_0} V(\mathbf{r})\, d\mathbf{r} \int_{-\infty}^{\infty} J(\omega)\, d\omega \left| \int_{S_A} \int_0^T E(\rho, t)\, e^{-i\omega t} H_\omega(\rho - \mathbf{r})\, dt\, d\rho \right|^2. \tag{3}$$

Utilizing the spectral representation

$$E(\rho, t) = \frac{1}{2\pi} \int_{-\infty}^{\infty} E(\rho, \omega)\, e^{-i\omega t} d\omega, \tag{4}$$

we convert (3) to a form convenient for physical interpretation of operations required for practical realization of Z:

$$Z = \frac{1}{2} \frac{k^2}{(2\pi)^2} \int_{S_0} V(\mathbf{r})\, d\mathbf{r} \int_0^T dt \left(\int_{-\infty}^{\infty} \int_{S_A} E(\rho, \omega)\, H_\omega(\rho - \mathbf{r})\, H(\omega)\, e^{i\omega t} d\omega\, d\rho \right)^2. \tag{5}$$

where $k = 2 \exp(-ixT/2) \sin(xT/2)\,(dx/x)$ is a real constant; and $H(\omega)$ is the frequency characteristic of the matched filter, whereby

$$|H(\omega)|^2 = |H_\Phi(\omega)|^2 |H_\text{д}(\omega)|^2 = J(\omega), \tag{6}$$

where $H_\text{д}(\omega)$ is the frequency characteristic of the equivalent filter of the detector, taking into account the dependence of the photodetector's sensitivity on frequency, defined as

$$|H_д(\omega)|^2 = \gamma(\omega)/(\hbar\omega), \tag{7}$$

($\gamma(\omega)$ is the quantum efficiency of the photodetector); and $H_f(\omega)$ is the frequency characteristic of a physically realizable matching filter.

Let us note that the transition from (3) to (5) is made on the assumption that $2\pi/T$ is much less than the bandwidths of the matching filter, $H_f(\omega)$, and of the equivalent filter of the detector, $H_d(\omega)$, and that the detector itself (an energy-sensitive recorder) includes three main elements: a filter, a squarer and an integrator.

The optimal processing arrangement realizing (5) can be represented in the form shown in fig 1. Telescope reflector 1 performs a Fourier transform operation of the type

$$E(\mathbf{r}, \omega) = \int_{S_A} E(\boldsymbol{\rho}, \omega) H_\omega(\boldsymbol{\rho} - \mathbf{r})\, d\boldsymbol{\rho};$$

matching filter $H_f(\omega)$, 2, matches the frequency characteristic, $H_d(\omega)$, of filter 4 and of detector 3 with the frequency characteristic, $J(\omega)$, of the received radiation; photodetector 3 together with matching filter 2, filter 4, squarer 5 and integrator 6 performs the operation

$$\int_0^T dt \left(\int_{-\infty}^{\infty} E(\mathbf{r}, \omega) H_ф(\omega) H_д(\omega) e^{i\omega t} d\omega \right)^2 = J_p(\mathbf{r})$$

and forms in the output the image to be registered of the object, $J_r(\mathbf{r})$. Then this image is scanned photometrically, is digitized and entered into the computer, 7, where in keeping with (5) from it is formed the value of quadratic functional Z.

This system realizes the magnitude of Z only as an average, and at each moment of time t the value of Z is random. This randomness is caused firstly by the randomness of the received light radiation, $E(\rho,t)$, and secondly, by the randomness of events of interaction between the light and the material of the light-sensitive screen of the photodetector and is characterized by probability distributions $P_{s+sh}(n)$ and $P_{sh}(n)$, where n is the number of events of interaction between the light and the material of the detector's photosensitive screen, and $P_{s+sh}(n)$ and $P_{sh}(n)$ are the probability distributions of the magnitude of Z in the presence and in the absence, respectively, of a useful signal from the object. Let us find these distributions.

2. Statistics of Photoreadings of Optimal Detection

Let us consider two possible cases: when processing is matched with the atmospheric channel, i.e., optimal processing is synthesized in the absence

of atmospheric distortion (and it actually is absent or is negligibly slight), and when processing is not matched with the atmospheric channel, i.e., optimal processing is synthesized in the absence of atmospheric distortion and it actually exists.

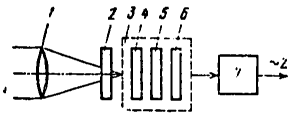

Figure 1.

Processing Matched with Atmospheric Channel

In this case the detected field, $E(\rho,t)$, represents a steady-state normal random process [2]. With a fixed field, $E(\rho,t)$, the distribution of the number of photoelectrons, n, in an optical detector with direct photodetection obeys Poisson's law

$$P[n/E(\rho, t)]=(Z^n/n!)\,e^{-Z} \tag{8}$$

with characteristic function

$$\psi(i\eta)=\exp\{Z[\exp(i\eta)-1]\}. \tag{9}$$

For the purpose of finding the characteristic function of magnitude Z and its probability distribution taking into account the Gaussian statistics of field $E(\rho,t)$, it is necessary to average (9) for all possible realizations of $E(\rho,t)$, and then from the averaged characteristic function of magnitude Z obtained to proceed to its probability distribution.

In the observation of an extended source of broadband radiation quadratic functional (5) can be represented in the form

$$Z=\frac{1}{2}\int_{S_A}\int_{S_A}\int_0^T\int_0^T E(\rho_1, t_1)\,E(\rho_2, t_2)\,V(\rho_1, \rho_2, t_1, t_2)\,dt_1\,dt_2\,d\rho_1\,d\rho_2, \tag{10}$$

where

$$V(\rho_1, \rho_2, t_1, t_2)=\frac{1}{(2\pi)^2}\int_{-\infty}^{\infty}\int_{S_0} V(\mathrm{r}, \omega)\exp[-i\omega(t_1-t_2)]\times$$
$$\times H_\omega(\rho_1-\mathrm{r})\,H_\omega^*(\rho_2-\mathrm{r})\,d\mathrm{r}\,d\omega, \tag{11}$$

and the correlation function of the detected field, $E(\rho,t)$, is determined by the relationship

$$R(\rho_1, \rho_2, t_1, t_2) = \frac{1}{(2\pi)^2} \int_{-\infty}^{\infty} \int_{S_0} J(\mathbf{r}, \omega) \exp[-i\omega(t_1 - t_2) H_\omega(\rho_1 - \mathbf{r}) \times \times H_\omega^*(\rho_2 - \mathbf{r})\, d\mathbf{r}\, d\omega + N_0 \delta(\rho_1 - \rho_2)\, \delta(t_1 - t_2). \tag{12}$$

Employing the procedure for finding the characteristic function of the quadratic functional for a Gaussian field in [3], we find that the characteristic function of magnitude Z has the form

$$\psi(u) = \langle \psi(i\eta) \rangle = \exp\left\{ \frac{1}{2} \int_{S_A} \int_0^T d\rho\, dt \int_0^u G(\rho, \rho, t, t; \lambda_0)\, d\lambda_0 \right\}, \tag{13}$$

where $u = x \exp(i\eta) - 1$ and function G is determined from the equation

$$G(\rho_1, \rho_2, t_1, t_2; \lambda_0) - \lambda_0 \int_{S_A} \int_0^T G(\rho_1, \rho, t_1, t; \lambda_0) \times \times \hat{V}(\rho, \rho_2, t, t_2)\, d\rho\, dt = \hat{V}(\rho_1, \rho_2, t_1, t_2), \tag{14}$$

where

$$\hat{V}(\rho_1, \rho_2, t_1, t_2) = \int_{S_A} \int_0^T V(\rho_1, \rho, t_1, t) R(\rho, \rho_2, t, t_2)\, d\rho\, dt. \tag{15}$$

Substituting (11) in (12) and (15) we find

$$\hat{V}(\rho_1, \rho_2, t_1, t_2) = \int_{-\infty}^{\infty} \int_{S_0} \tilde{V}(\mathbf{r}, \omega) e^{-i\omega(t_1 - t_2)} H_\omega(\rho_1 - \mathbf{r}) H_\omega^*(\rho_2 - \mathbf{r})\, d\mathbf{r}\, d\omega, \tag{16}$$

where

$$\tilde{V}(\mathbf{r}, \omega) = V(\mathbf{r}, \omega)(N_0/4\pi^2)[q(\mathbf{r}, \omega) + 1]; \tag{17}$$

$$q(\mathbf{r}, \omega) = J(\mathbf{r}, \omega)/(2\pi N_0) \tag{18}$$

is the signal-to-noise ratio in the space-time resolution element of the processing system.

According to the recommendations in [3] we seek a solution to equation (14) in the form

$$G(\rho_1, \rho_2, t_1, t_2; \lambda_0) = \int_{-\infty}^{\infty} \int_{S_0} G(\mathbf{r}, \omega; \lambda_0) \exp[-i\omega(t_1 - t_2)] \times \\ \times H_\omega(\rho_1 - \mathbf{r}) H_\omega^*(\rho_2 - \mathbf{r})\, d\mathbf{r} \cdot d\omega; \tag{19}$$

then, as is not hard to verify, with high T and S_A we get

$$G(\mathbf{r}, \omega; \lambda_0) = \tilde{V}(\mathbf{r}, \omega)/[1 - \lambda_0 q(\mathbf{r}, \omega)], \tag{20}$$

$$G(\rho, \rho, t, t; \lambda_0) = \int_{-\infty}^{\infty} \int_{S_0} \frac{G(\mathbf{r}, \omega; \lambda_0)}{(\lambda R)^2}\, d\mathbf{r} \cdot d\omega. \tag{21}$$

Substituting (20) in (21) and (21) in (13), after integrating in terms of λ_0 we get the characteristic function of magnitude Z in the presence of a useful signal:

$$\psi_{c+m}(u) = \exp\left\{-\frac{TS_A}{4\pi} \int_{-\infty}^{\infty} \int_{S_0} \frac{1}{(\lambda R)^2} \ln[1 - uq(\mathbf{r}, \omega)]\, d\mathbf{r} \cdot d\omega\right\}. \tag{22}$$

In the absence of a useful signal from the object, i.e., when instead of (12) we have

$$R(\rho_1, \rho_2, t_1, t_2) = N_0 \delta(\rho_1 - \rho_2)\, \delta(t_1 - t_2), \tag{23}$$

after similar transforms we get the characteristic function of magnitude Z :

$$\psi_m(u) = \exp\left\{-\frac{TS_A}{4\pi} \int_{-\infty}^{\infty} \int_{S_0} \frac{1}{(\lambda R)^2} \ln\left[1 - u\frac{q(\mathbf{r}, \omega)}{1 + q(\mathbf{r}, \omega)}\right] d\mathbf{r} \cdot d\omega\right\}. \tag{24}$$

Generally it is not possible to obtain an expression for probability distributions corresponding to characteristic functions (22) and (23) without resorting to approximations of $q(\mathbf{r},\omega)$. Approximating function $q(\mathbf{r},\omega)$ by a square-type curve in the processing system's transmission band of $\Delta\omega = 2\pi\Delta f$ and assuming that the object has a uniform spatial distribution of intensity with regard to its projection, S_0 , on the picture plane, we get

$$\psi_{c+m}(u) = \exp\{-mM \ln[1 - uq]\}, \tag{25}$$

$$\psi_{ш}(u) = \exp\left\{-mM \ln\left[1 - u\frac{q}{1+q}\right]\right\}, \tag{26}$$

where $m = T\Delta f$ is the number of time resolution elements (degrees of freedom) of the processing system and $M = S_0 S_A/(\lambda R)^2$ is the number of space resolution elements of the processing system.

Taking into account the quantum effects of registration, (7) , and the Poisson statistics for the number of dark photoelectrons of the recorder, n_t , substituting in (25) and (26) $u = in - 1$ by $u - 1$, finally we get the generating function of magnitude Z in the presence and absence of a useful signal:

$$\psi_{c+ш}(u) = [1-(u-1)\,q]^{-mM} \exp[(u-1)\,\bar{n}_т], \tag{27}$$

$$\psi_{ш}(u) = \left[1 - (u-1)\frac{q}{1+q}\right]^{-mM} \exp\left[(u-1)\,\bar{n}_т\right], \tag{28}$$

where $\bar{n}_t$ is the mean number of dark photoelectrons of the detector.

We convert (27) to the form

$$\psi_{c+ш}(v) = \frac{e^{-\bar{n}_т}}{(1+q)^{mM}} \frac{e^{vx}}{(1-v)^{mM}}, \tag{29}$$

where the following symbols are introduced:

$$v = uq/(1+q); \quad x = \bar{n}_т\,(1+q)/q. \tag{30}$$

Then based on determination of the generating function we have

$$\sum_{n=0}^{\infty} P_{c+ш}(n)\,v^n = \frac{e^{-\bar{n}_т}}{(1+q)^{mM}}\left(1 + v + \frac{v^2}{2!} + \dots\right)^{mM}\left(1 + vx + \frac{(vx)^2}{2!} + \dots\right), \tag{31}$$

whence, employing the familiar equation for the generating function of a generalized orthogonal Laguerre polynomial [4]

$$\sum_{n=0}^{\infty} L_n^{\alpha}(x)\,u^n = (1-u)^{-(\alpha+1)} \exp\left\{\frac{xu}{u-1}\right\}, \tag{32}$$

after not too complicated transforms we get

$$P_{c+ш}(n) = \frac{e^{-\bar{n}_т}}{(1+q)^{mM}}\left[L_0^{mM-1}(0)\frac{x^n}{n!} + L_1^{mM-1}(0)\frac{x^{n-1}}{(n-1)!} + \cdots + L_n^{mM-1}(0)\right]\left(\frac{q}{1+q}\right)^n. \tag{33}$$

Whence, taking (30) into account, we finally get the probability distribution for magnitude Z :

in the presence of a useful signal

$$P_{c+ш}(n)\,e^{-\bar{n}_т}\left[\frac{mM}{mM+(\bar{n}_c+\bar{n}_\Phi)}\right]^{mM}\left[\frac{\bar{n}_c+\bar{n}_\Phi}{mM+(\bar{n}_c+\bar{n}_\Phi)}\right]^n \times \times \sum_{l=0}^{n} L_{n-l}^{mM-1}(0)\frac{\left[\bar{n}_т\frac{mM+(\bar{n}_c+\bar{n}_\Phi)}{\bar{n}_c+\bar{n}_\Phi}\right]^l}{l!}, \tag{34}$$

and in the absence of a useful signal

$$P_ш(n) = e^{-\bar{n}_т}\left[\frac{mM}{mM+\bar{n}_\Phi}\right]^{mM}\left[\frac{\bar{n}_\Phi}{mM+\bar{n}_\Phi}\right]^n \sum_{l=0}^{n} L_{n-l}^{mM-1}(0)\frac{\left[\bar{n}_т\frac{mM+\bar{n}_\Phi}{\bar{n}_\Phi}\right]^l}{l!}, \tag{35}$$

where

$$\bar{n}_c = mMq^2/(1+q);\ \bar{n}_\Phi = mMq/(1+q); \tag{36}$$

$\bar{n}_s$ and $\bar{n}_f$ are the mean number of signal and background photoelectrons in the image of the extended object during processing period T in transmission band Δf .

Expressions (34) and (35) represent highly general equations for the probability distribution of quadratic functional Z in (10) taking into account the Gaussian statistics of the detected field, $E(\rho,t)$, the quantum effects of registration, the Poisson statistics of dark currents and any m , M and q .

In the particular case of $mM \gg 1$ it is possible to employ an asymptotic expansion of the characteristic function of the type

$$\langle \psi_{c+ш}(i\eta)\rangle = \exp\left[(e^{i\eta}-1)\,(qmM+\bar{n}_т)\right], \tag{37}$$

whereby the statistics of photoreadings of magnitude Z obey the Poisson distribution law

$$P_{c+ш}(n) = \frac{(\bar{n}_c+\bar{n}_\Phi+\bar{n}_т)^n}{n!}\exp\left[-(\bar{n}_c+\bar{n}_\Phi+\bar{n}_т)\right], \tag{38}$$

$$P_{ш}(n) = \frac{(\bar{n}_\Phi+\bar{n}_т)^n}{n!}\exp\left[-(\bar{n}_\Phi+\bar{n}_т)\right]. \tag{39}$$

The result obtained refines the conditions for the applicability of the Poisson approximation, which consists in fulfillment of the inequalities

$$n_т+n_\Phi \ll mM;\ \bar{n}_c+\bar{n}_\Phi \ll mM. \tag{40}$$

In another particular case, when it is possible to disregard dark currents ($\bar{n}_т = 0$) in (34) and (35), the statistics of photoreadings of magnitude Z obey a negative binomial distribution of the type

$$P_{c+ш}(n) = \frac{(n+mM-1)!}{(mM-1)!\,n!}\left[\frac{mM}{mM+(\bar{n}_c+\bar{n}_\Phi)}\right]^{mM}\left[\frac{\bar{n}_c+\bar{n}_\Phi}{mM+(\bar{n}_c+\bar{n}_\Phi)}\right]^n, \tag{41}$$

$$P_{ш}(n) = \frac{(n+mM-1)!}{(mM-1)!\,n!}\left[\frac{mM}{mM+\bar{n}_\Phi}\right]^{mM}\left[\frac{\bar{n}_\Phi}{mM+\bar{n}_\Phi}\right]^n, \tag{42}$$

where the property of the Laguerre polynomial is used:

$$L_n^\alpha(0) = \binom{n+\alpha}{n}.$$

Thus, we have obtained and studied probability distributions of quadratic functional Z in (10), synthesized in the absence of atmospheric distortion, for the case when processing is matched with the atmospheric channel. Let us consider how the statistical characteristics of the optimal detection under consideration change in the presence of atmospheric phase distortion, $\theta(\rho,\omega)$.

Processing not Matched with Atmospheric Channel

In this case, with a fixed field, $E(\rho,t)$, magnitude Z in (10) is distributed according to Poisson equation (8) with characteristic function (9). But now it is necessary to average this characteristic function twice. First, with a fixed phase of atmospheric fluctuations, as before it is necessary to average in terms of Gaussian field $E(\rho,t)$, and then it is necessary to average the characteristic function obtained for a Gaussian field with a fixed phase in terms of the Gaussian atmospheric phase, $\theta(\rho,\omega) = (\omega/c)S(\rho)$. After this it is possible to find the probability distribution of magnitude Z from the twice averaged characteristic function.

With a fixed phase of atmospheric fluctuations, $\theta(\rho,\omega)$, the correlation function of Gaussian field $E(\rho,t)$, unlike (12), has the form

$$R(\rho_1, \rho_2, t_1, t_2) = \frac{1}{(2\pi)^2} \int_{-\infty}^{\infty} \int_{S_0} J(\mathbf{r}, \omega) \exp\left\{i \frac{\omega}{c} [S(\rho_1) - S(\rho_2)]\right\} \times$$
$$\exp[-i\omega(t_1 - t_2)] H_\omega(\rho_1 - \mathbf{r}) H_\omega^*(\rho_2 - \mathbf{r})\, d\mathbf{r}\, d\omega + N_0 \delta(\rho_1 - \rho_2)\, \delta(t_1 - t_2). \tag{43}$$

Having employed the procedure described for finding the characteristic function of quadratic functional Z for Gaussian field $E(\rho,t)$, we get

$$\psi_{c+m}[u/S(\rho)] = \exp\left\{-\frac{TS_A}{4\pi} \frac{1}{S_A} \int_{S_A} d\rho \int_{S_0} d\mathbf{r} \int_{-\infty}^{\infty} d\omega \frac{1}{(\lambda R)^2} \times \right.$$
$$\times \ln\left[1 - u\left(\frac{q(\mathbf{r},\omega)}{1+q(\mathbf{r},\omega)} + \frac{q^2(\mathbf{r},\omega)}{1+q(\mathbf{r},\omega)} \exp\left[-i\frac{\omega}{c} S(\rho)\right] \frac{1}{S_A} \times \right.\right.$$
$$\left.\left.\left. \times \int_{S_A} \exp\left[i\frac{\omega}{c} S(\rho_1)\right] d\rho_1\right)\right]\right\}, \tag{44}$$

and we get the generating function for magnitude Z with a fixed phase by replacing in (44) u by $u - 1$:

$$\psi_{c+m}[u/S(\rho)] = \exp\left\{-\frac{TS_A}{4\pi} \frac{1}{S_A} \int_{S_A} d\rho \int_{S_0} d\mathbf{r} \int_{-\infty}^{\infty} d\omega \frac{1}{(\lambda R)^2} \times \right.$$
$$\times \ln\left[1 - (u-1)\left(\frac{q(\mathbf{r},\omega)}{1+q(\mathbf{r},\omega)} + \frac{q^2(\mathbf{r},\omega)}{1+q(\mathbf{r},\omega)} \exp\left[-i\frac{\omega}{c} S(\rho)\right] \frac{1}{S_A} \times \right.\right.$$
$$\left.\left.\left. \times \int_{S_A} \exp\left[i\frac{\omega}{c} S(\rho_1)\right] d\rho_1\right)\right]\right\}. \tag{45}$$

Before proceeding to averaging (45) for the ensemble of realizations of Gaussian phase $\theta(\rho,\omega) = (\omega/c)S(\rho)$, we note that when the area of the correlation cell of the distorted atmospheric field, $S_\theta = \pi R_\theta^2/4$, is greater than the area of the telescope's receiving aperture, $S_A = \pi D^2/4$ (the condition for good atmospheric "viewing"), function $\exp[i(\omega/c)S(\rho_1)]$ can be taken out from behind the integral sign in (45); then it is not hard to verify that (44) agrees with (22), and the statistics of photoreadings of magnitude Z practically do not depend on the presence of a turbulent atmosphere in front of the telescope's aperture.

Let us consider the most interesting and often practically realized case when fit into the large receiving aperture of the telescope are many correlation cells of an atmosphere-distorted light field ($S_\theta \ll S_A$). It is not difficult to verify that here the second term in (45) is substantially smaller than the first. Employing expansion $\ln(1-x) \sim -x$, generating function (45) can be represented in the form

$$\psi_{c+m}[u/S(\rho)] = \exp\left\{-\frac{TS_A}{4\pi}\int_{S_0} dr \int_{-\infty}^{\infty} d\omega \frac{1}{(\lambda R)^2} \ln\left[1-(u-1)\frac{q(r,\omega)}{1+q(r,\omega)}\right]+\right.$$
$$+\frac{TS_A}{4\pi}\int_{S_0} dr \int_{-\infty}^{\infty} d\omega \frac{1}{(\lambda R)^2} \frac{(u-1)\frac{q^2(r,\omega)}{1+q(r,\omega)}}{1-(u-1)\frac{q(r,\omega)}{1+q(r,\omega)}} \frac{1}{S_A^2} \times$$
$$\left.\int_{S_A}\int_{S_A} \exp\left\{i\frac{\omega}{c}[S(\rho_1)-S(\rho_2)]\right\} d\rho_1 d\rho_2\right\}. \tag{46}$$

We designate by y the value

$$y = \frac{1}{S_A^2}\int_{S_A}\int_{S_A} \exp\left\{i\frac{\omega}{c}[S(\rho_1)-S(\rho_2)]\right\} d\rho_1 d\rho_2 \tag{47}$$

and we expand generating function (46) in the vicinity of point <y> into a Taylor series up to quadratic terms:

$$\psi(y) = \psi(\langle y\rangle) + \psi'(y)(y-\langle y\rangle) + 1/2\,\psi''(y)(y-\langle y\rangle)^2 + \ldots \tag{48}$$

On the condition of a low value of the third term of expansion (48), which, as it is not difficult to verify, is fulfilled in the case considered,

$$N = S_A/S_\theta \gg 1, \tag{49}$$

we get the equation

$$\langle \psi(y) \rangle = \psi(\langle y \rangle), \tag{50}$$

which we also employ in averaging (46). Then after averaging (46) we get the generating function of quadratic functional Z (cf. (10)) in the presence of atmospheric phase fluctuations in the form

$$\psi_{c+m}(u) = \exp\left\{ -\frac{TS_A}{4\pi} \int_{S_0} dr \int_{-\infty}^{\infty} d\omega \frac{1}{(\lambda R)^2} \ln\left[1 - (u-1) \frac{q(r, \omega)}{1+q(r, \omega)} \right] + \right.$$
$$+ \frac{TS_A}{4\pi} \int_{S_0} dr \int_{-\infty}^{\infty} d\omega \frac{1}{(\lambda R^2)} \frac{(u-1)\frac{q^2(r, \omega)}{1+q(r, \omega)}}{1-(u-1)\frac{q(r, \omega)}{1+q(r, \omega)}} \frac{1}{S_A^2} \times$$
$$\left. \times \int_{S_A} \int_{S_A} \exp\left\{ -\sigma_\theta^2 \left[1 - \exp\left(-\frac{|\rho_1 - \rho_2|^2}{a_\theta^2} \right) \right] \right\} d\rho_1 \, d\rho_2 \right\}, \tag{51}$$

where a_θ is the space correlation distance of atmospheric phase fluctuations; and σ_θ^2 is their variance, and the space correlation distance of the atmosphere-distorted field, R_θ, is determined by their ratio: $R_\theta = a_\theta/\sigma_\theta$.

If now, as previously, is employed an approximation of function $q(r,\omega)$, then with condition (49), after not too complicated transforms, generating function (51) can be represented in the form

$$\psi_{c+m}(u) = \left[1 - (u-1)\frac{q}{1+q} \right]^{-mM} \exp\left\{ mM \frac{q}{N} \frac{(u-1)\frac{q}{1+q}}{1-(u-1)\frac{q}{1+q}} \right\}, \tag{52}$$

and taking Poisson dark currents into account,

$$\psi_{c+m}(u) = e^{-\bar{n}_\tau} \left(\frac{1+q}{1+2q} \right)^{mM} \exp\left\{ -mM \frac{q}{N} \right\} [1-z]^{mM} \times$$
$$\times \exp\left\{ \frac{x}{z-1} \right\} \exp\{zx'\}, \tag{53}$$

where the following symbols are introduced

$$z = u\frac{q}{1+2q}; \quad x = -\left(\frac{1+q}{1+2q} \right) mM \frac{q}{N}; \quad x' = \bar{n}_\tau \frac{1+2q}{q}. \tag{54}$$

Then employing the equation for the generating function of the generalized Laguerre polynomial

$$\sum_{n=0}^{\infty} L_n^{\alpha}(x) z^n e^{-x} = (1-z)^{-(\alpha+1)} e^{xz/(z-1)}, \tag{55}$$

which can be obtained easily from (32), and taking (31) and (33) into account, after not too complicated transforms we finally get the probability distribution for magnitude Z in (10):

in the presence of a useful signal

$$P_{c+m}(n) = e^{-\left[\bar{n}_T + \frac{\bar{n}_c}{1+\frac{\bar{n}_\Phi}{mM}}\right]} \left[\frac{mM}{mM+\bar{n}_\Phi}\right]^{mM} \left[\frac{\bar{n}_\Phi}{mM+\bar{n}_\Phi}\right]^n \times$$
$$\times \sum_{l=0}^{n} L_{n-l}^{mM-1}\left[-\frac{\bar{n}_c}{\left(1+\frac{\bar{n}_\Phi}{mM}\right)\frac{\bar{n}_\Phi}{mM}}\right] \frac{\left[\bar{n}_T\left(\frac{mM+\bar{n}_\Phi}{\bar{n}_\Phi}\right)\right]^l}{l!}, \tag{56}$$

and in its absence

$$P_m(n) = e^{-\bar{n}_T}\left[\frac{mM}{mM+\bar{n}_\Phi}\right]^{mM}\left[\frac{\bar{n}_\Phi}{mM+\bar{n}_\Phi}\right]^n \times$$
$$\times \sum_{l=0}^{n} L_{n-l}^{mM-1}[0] \frac{\left[\bar{n}_T\left(\frac{mM+\bar{n}_\Phi}{\bar{n}_\Phi}\right)\right]^l}{l!}, \tag{57}-(35)$$

where

$$\bar{n}_c = mMq_A q/(1+q); \quad \bar{n}_\Phi = mMq(1+q), \tag{58}$$

and $q_A = q/N$ is the signal-to-noise ratio in the space-time resolution element of the processing system with the presence of atmospheric distortion. Let us note that in the particular case when $n_s + n_\Phi \ll mM$, distributions (56) and (57) are approximated by Poisson distributions similar to (38) and

(39), with the only difference that now $\bar{n}_s$ and $\bar{n}_f$ are determined not from (40), but from (58).

3. Conclusion

And so, as a result of investigations made by taking into account quantum effects and registration noise, it has been found that the statistics of photoreadings of optimal detection of incoherent broadband radiation in the presence of a useful signal obey two different distribution laws: when processing is matched with the atmospheric channel--by a distribution law of type (34), and when processing and the atmospheric channel are mismatched--by a distribution law of type (56); in the absence of a useful signal in both cases the statistics of magnitude Z obey a distribution law of type (35).

Let us note that in the particular case of detection of monochromatic radiation ($m = 1$) in the absence of atmospheric phase fluctuations ($N = 1$) probability distribution (34) agrees with the distribution obtained under similar conditions in [5]. Based on a qualitative comparison of distributions (34) and (56) obtained, it is possible to state that the presence of atmospheric distortion alters the statistics of photoreadings of optimal detection and worsens the energy characteristics of distribution (56) thereby obtained, lowering the signal-to-noise ratio in the processing system's resolution element. This testifies to the need to take into account the results obtained here in estimating the potential capacity for the optimal reception of incoherent broadband radiation under conditions of atmospheric "viewing."

Bibliography

1. Kuriksha, A.A. "Kvantovaya optika i opticheskaya lokatsiya" [Quantum Optics and Optical Finding], Moscow, Sovetskoye Radio, 1973.

2. Bakut, P.A., Sviridov, K.N., Troitskiy, I.N. and Ustinov, N.D. RADIOTEKHNIKA I ELEKTRONIKA, No 8, 1503 (1979).

3. Bakut, P.A. et al. "Voprosy statisticheskoy teorii radiolokatsii" [Problems in the Statistical Theory of Radar], Moscow, Sovetskoye Radio, 1963, Vol 1.

4. Beytman, G. and Erdeyn, A. "Vysshiye transtsendentnyee funktsii" [Higher Transcendental Functions], Vol 2, Moscow, Nauka, 1966.

5. Goodman, J.W. PROC. IEEE, 53, 1688 (1965).

CSO: 1862
8831

LASERS AND MASERS

UDC 621.373.826.038.823

INVESTIGATION OF CHARACTERISTICS OF A FAST-FLOW CONTINUOUSLY OPERATING CO_2 LASER EXCITED BY A SELF-MAINTAINED DIRECT-CURRENT DISCHARGE

Moscow KVANTOVAYA ELEKTRONIKA in Russian Vol 6 No 9, Sep 79 pp 1953-1959
manuscript received 22 Jan 79

[Article by A.G. Basiyev, V.I. Blokhin, V.A. Yepishov, V.N. Kuz'min, V.A. Myslin, S.V. Pashkin and V.N. Shulakov, Institute of Atomic Energy imeni I.V. Kurchatov, Moscow]

[Text] The results are given of experimental investigations of individual units of a mockup of a fast-flow electric-discharge continuously operating CO_2 laser operating with a mixture of air and CO_2 with a pressure of about 100 mm Hg. A discharge chamber efficiency of about 0.7 is produced and gain values of up to one percent per centimeter.

1. For the purpose of solving a number of technological problems it is possible to use a fast-flow continuous CO_2 laser excited by a self-maintained direct-current discharge. Restriction on the power of these lasers is associated primarily with worsening of the stability of the discharge with an increase in pressure of the working medium and of the gap between electrodes [1-3]. These difficulties are eliminated to a considerable extent with a fast flow of the working mixture in a system with mutually perpendicular directions of the gas flow, electric current and axis of the cavity [4].

The employment of mixing of carbon dioxide gas beyond the area of the cavity makes it possible to create a laser system effectively operating at elevated pressures of the working medium. It is economically feasible to employ as the accumulator of vibrational energy nitrogen of the air, whereby the water contained in the air makes it possible to quench the lower laser level of the CO_2 molecule and to refrain from using helium [5].

The purpose of this paper has been an experimental verification of the efficiency of this arrangement at elevated pressures and a search for optimal solutions for the design of its individual units.

2. A diagram of the experimental unit is shown in fig 1. Its key units are the discharge chamber, 1, where the excitation of the vibrational levels of

molecules of nitrogen takes place, a collector, 2, for mixing CO_2 into the excited medium, and a cavity, 3. The flow of air was created by a two-stage ejector system, 4, and its rate of flow was set by Venturi-type nozzles, 5, installed in front of the inlet of the discharge chamber. The temperature of the air in the inlet equaled about 20°C, with a relative humidity of 60 to 80 percent.

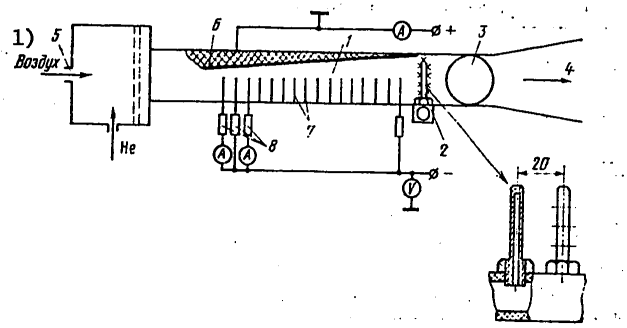

Figure 1. Diagram of Experimental Unit

Key:
1. Air

The discharge zone of chamber 1 is formed by an anode, 6, in the form of a copper plate with an interspaced cathode, 7, consisting of steel pins 2 to 4 mm in diameter, arranged in checkerboard fashion. The length of the pins and the interelectrode gap could be varied. Each pin was connected to the power supply via a decoupling ballast resistor, 8, rated at 4 to 10 kΩ. The characteristic geometrical dimensions of the discharge chamber were: the length of the electrode system in relation to air flow, L = 24 cm ; its width, B = 10 cm ; distance between anode and cathode board, H = 4 to 5 cm ; distance from ends of pins to surface of anode, h = 1 to 3 cm ; number of pins, n = 160 (m = 16 rows along the flow and k = 10 in a row transverse to the flow).

3. At the first stage the main problem was optimization of the discharge chamber with regard to the power, W , contributable to the gas flow. Measurements were made of parameters of the gas flow--statistical and total pressure at different points in the chamber--and of electrical magnitudes--current and voltage and their distribution by pin.

In the table are given the results of some experiments with various configurations of the discharge zone.

Table 1.

H/h	1) G, г/с	2) $p_{вх}$, мм рт. ст.	3) $p_{вых}$, мм рт. ст.	4) $v_{вх}/v_{вых}$, м/с	5) W, кВт	6) W/G, Дж/г
5,0/2,7	90	57	35	210/310	19	210
4,0/2,5	90	84	48	210/250	17	190
5,0/3—3,6	90	67	57	125/140	15	170
5,0/3—3,6	120	75	40	200/300	16	140
4,0/1,1—1,8	90	135	105	220/290	2,7	300

Note: G is the rate of flow of the gas; v_{vkh} and v_{vykh} are the velocity of the gas at the inlet and outlet of the discharge chamber.

Key:
1. G , g/cm
2. p_{vkh} , mm Hg
3. p_{vykh} , mm Hg
4. v_{vkh}/v_{vykh} , m/s
5. W , kW
6. W/G , J/g

It is obvious from this table that the maximum power contributed to the diffused discharge was obtained when operating with a discharge chamber with H = 4 cm and an interelectrode gap of 1.1 cm at the beginning and of 1.8 cm at the end of the chamber. Here the power per unit volume (W/(LBH)) reached on average 30 W/cm^3 for the gas space and approximately 70 W/cm^3 for the interelectrode gap.

In fig 2 for this electrode configuration are given the relative distribution of current in terms of rows of pins, $\bar{I}_i = I_i/I_\Sigma$, and ratios of the mean electric field strength in terms of the length of the chamber to the static pressure, E/p . It is obvious that with a growth in contributed power there is an increase in nonuniformity in the distribution of current by rows of pins, and the value of E/p falls more rapidly downstream. This can be explained both by the reduction in the gas's density on account of its heating, and by the increase in concentration of excited molecules and frequencies of collisions of the second kind between electrons and molecules. It should be mentioned that equalizing the current distribution for rows of electrodes by changing the values of ballast resistors does not produce a noticeable increase in contributed power.

A certain percentage of the pumping energy in the electric discharge is used to increase the translational temperature of the gas. The effectiveness of this process was determined by two methods. First measurements were made of the temperature of the gas in the center of the stream beyond the discharge, by means of Chromel-Alumel thermocouples. These measurements showed that

with a contributed power level of W/G = 300 J/g the temperature of the gas at the center at a distance of approximately 2 cm from the last row of pins was not greater than 100°C, i.e., the percentage of energy used to heat the air equaled not greater than 30 percent of the total energy contributed to the flow. However, because of possible incorrectness of measurements of temperature of the gas by means of thermocouples (e.g., resulting from their catalytic nature, which generally speaking overstates the true value of the gas's temperature), balancing estimating calculations were made of the chamber's efficiency (cf. below) from measured values of the total and static pressure in different sections of the chamber. The mean bulk temperature was estimated by the change in pressure in modes with a discharge and without one.

It was found that the rate of flow of gas through the pin area dropped from approximately 40 percent of the total rate of flow at the beginning to five percent at the end of the chamber, and that the mean bulk temperature of the gas directly behind the discharge zone did not exceed 70°C under the most strained conditions, although the temperature of the gas passing between pins could reach 400°C. Thus, the experiments have demonstrated that the percentage of energy going toward heating the gas in the discharge chamber does not exceed to 20 to 30 percent with contributed power of up to 300 J/g.

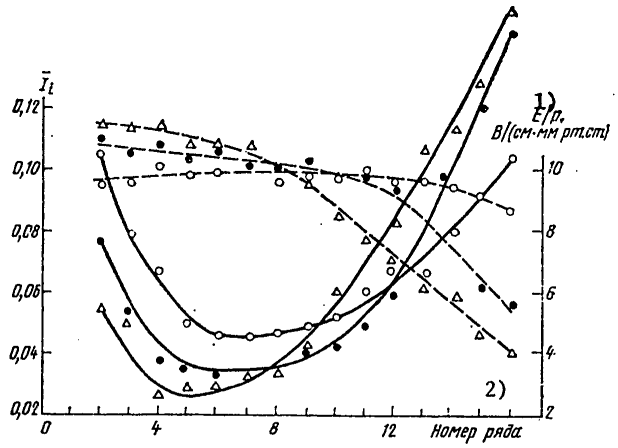

Figure 2. Distribution of Current, $\bar{I}_i$, (Solid Lines) and of Mean Normalized Field Strength, E/p, (Dotted Lines) for Rows of Electrodes Along the Air Stream with I_r = 6 (White Dots), 10 (Black Dots) and 15 A (Triangles)

Key:
1. E/p, W/(cm·mm Hg)
2. Number of row

Let us analyze the reasons for heating of the gas in the chamber. It can be caused first by bulk processes occurring directly in the gas discharge and associated with the flow of current and secondly by losses near electrodes and thirdly by the relaxation of vibrational energy in the discharge zone. According to [5] the heating of gas according to the first mechanism equals about 10 percent. With regard to the second mechanism it can be assumed that, since the magnitude of voltage drops near electrodes is most likely not greater than 500 V (with air and the specific electrode material) and the total voltage applied to the electrodes equals 2.5 to 3.0 kV, the contribution of losses near electrodes to heating of the gas is not greater than 20 percent. However it is necessary to take into account the fact that a great percentage of the heat can go toward heating the walls of the discharge chamber and that the heated gas is concentrated chiefly in the layers near electrodes and in the stream behind the pins. The relaxation of vibrational energy in the air stream takes place chiefly in molecules of water. With a temperature of 20°C and relative humidity of 0.6 to 0.8 as much as two percent H_2O is contained in the air. Assuming the reaction rate for the vibrational relaxation of nitrogen in water to equal $k_r = 10^{-15}$ cm^3/s [6], we find that with $p =$ $= 100$ mm Hg , $T = 300°K$ and $v = 200$ m/s , the relaxation length equals $L_r \sim 3$ m . Hence it is obvious that relaxation in water in our case gives a contribution to heating of the gas on the order of a few percent. With a chamber length of $L = 22$ cm and a distance from its section to the axis of the cavity of 5 to 8 cm, losses of vibrational energy on account of relaxation in moist air can reach five to 10 percent (for comparison, in a chamber with plate-type cathode elements with lower operating rates of flow, relaxation losses equaled with $p = 100$ mm Hg about 40 percent [7]). In the intensification of relaxation a certain role can be played by not too great a portion of the hot air entering the main stream from the zone occupied by the pins. Thus, an analysis of thermal heating of the air has shown that the heating of gas in the main stream equals not greater than 30 percent, which is in accord with the measurement results. If used for the efficiency of the discharge chamber is the ratio of the share of electric power supplied to the discharge and not going toward heating of the gas, to the entire power supplied to the discharge, then the efficiency of a pin-type chamber with $r_{st} = 100$ mm Hg for air and with $v = 200$ m/s proves to equal $\eta = 0.7$.

4. The next stage in investigation was an estimate of the operating quality of the mixing system by means of measuring parameters of the active medium in the area of the cavity. CO_2 was mixed directly beyond the discharge zone. The CO_2 delivery system must make possible as fine spraying as possible in order to speed up mixing of the gases, and on the other hand it must not severely encumber the flow.

Two designs of sprayers for gaseous carbon dioxide were made and tested. The first was in the form of a comb of Teflon tubes spaced at 20 mm across the flow. Each tube had four holes on each side measuring 0.5 mm in diameter and spaced 10 mm apart and one opening at the end 1 mm in diameter. The holes were so situated that the jets of CO_2 were directed across the excited air. The pressure of CO_2 in the distributing system equaled 1 to 6 atm.

Another sprayer design was in the form of a comb of thin-walled brass tubes 2 mm in diameter, spaced 10 mm apart across the excited air and spanning the entire cross section of the discharge chamber. The holes for supplying CO_2 had a diameter of 0.2 mm and were spaced 10 mm apart along the side walls of the tubes.

Mixing quality was rated by measuring the spatial distribution of the gain, $K_u = J/J_0$, of the weak signal, J_0, of a master CO_2 laser. A two-way measuring system was used (fig 3). The power of the master laser's output emission was not greater than 1 W, which made it possible to measure in the straight-line section of the thermocouple detector's characteristics. The maximum error in measuring the increase in radiation intensity was not greater than 10 percent.

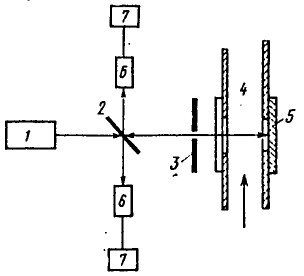

Figure 3. System for Measuring Gain: 1--master CO_2 laser; 2--semi-transparent plate; 3--diaphragm; 4--active medium; 5--mirror; 6--attenuators; 7--radiation detectors

In fig 4a are given values of the gain for two operations as a function of the distance to the anode with a distance downstream from the Teflon collector of $x = 2.5$ cm for different discharge currents. The bulk percentage of CO_2 equaled 10 percent in proportion to the air. It is obvious from the graph that with a change in current from 6 to 15 A the gain, K_u, for the inter-electrode gap remains almost constant, whereby the maximum value of $K_u = 1.22$ is reached with $I = 10$ A.

In fig 4b are given dependences of the gain, K_u, on the distance to the Teflon collector with different concentrations of CO_2 and a unit energy contribution to the gas stream of $W/G \simeq 200$ J/g. With an increase in CO_2 concentration, at distances of approximately 15 to 50 mm the gain grows monotonically, and then, at great distances from the collector with $[CO_2] >$ five percent, it drops. This, in our opinion, is related to the competition of two factors: the mixing of gases and the relaxation of vibrational energy. The absolute value of the gain as a maximum equals $K_0 = (1/2B) \ln K_u \simeq 1\%/\text{cm}$.

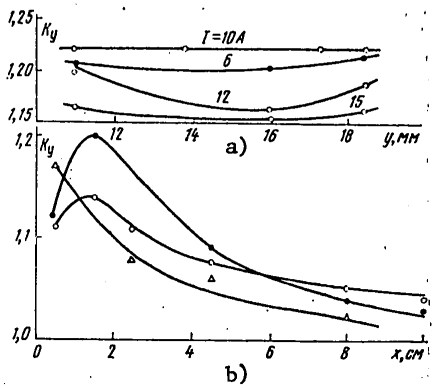

Figure 4. Distribution in Gain: a--across the gas stream at a distance of 2.5 cm downstream from the Teflon collector; b--along the stream at its center section with a unit energy contribution of 200 J/g and CO_2 concentrations of 5 (triangles), 10 (white dots) and 15 percent (black dots)

In going from one series of experiments to another is observed a considerable spread in gain of the weak signal, K_u, at a distance of up to 4 cm from the collector, although the general patterns are maintained within the range of a series. This is probably explained by the fact that the points lie in a zone of intense turbulent mixing of jets of CO_2 with the excited air, the geometry of which is crucial for experimental conditions and is hard to reproduce.

Working with different collector designs shows a strong dependence of the medium's gain on the system for supplying CO_2. The metal collector described above produces, with a CO_2 concentration greater than 7.5 percent at a distance of 6 cm from the collector, a considerably greater gain than a Teflon collector, which speaks for its better mixing quality. With low mean concentrations of CO_2 (approximately five percent) signal gains in both cases are slight and have close values. In fig 5 are given dependences of K_u on current for these collectors with $x = 2$ to 2.5 cm and $[CO_2] = 7.5$ percent.

It is possible to rate the operation of a CO_2 mixing system by measuring gain in terms of two characteristics: of the drop in K_u downstream and of the absolute value of K_u in the area of the cavity.

The value of the gain is closely related to the population density of energy levels of CO_2 molecules. Since collision broadening with our pressure is greater than the Doppler breadth, the gain, K_0, is given by the equation in [8]:

$$K_0 = \frac{540}{T} \frac{n_{001} - n_{100}}{N \Sigma [i] A_i},$$

where T is the temperature of the gas in °K; N is the total density of molecules in the mixture; and $[i]A_i$ characterizes the role of different components of the mixture. In our case $[i]A_i = 0.75$. Assuming that the lower laser level is populated at the gas temperature and the upper at the vibrational temperature of nitrogen (i.e., $n_{001} \gg n_{100}$), we get $K_0 \approx (0.7/T)[CO_2]\eta(W/g)[cm^{-1}]$.

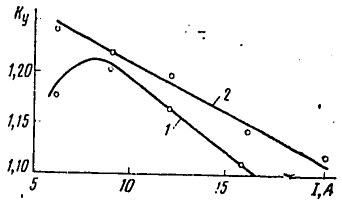

Figure 5. Distribution of K_u for Stream Behind Teflon (1) and Metal (2) Collectors

Taking into account the error in determination of the discharge efficiency and the temperature of the gas, it can be assumed that the absolute value of the gain in a homogeneous medium must equal under our conditions $K_0 \approx 0.1[CO_2](W/g)$ [%/cm]. Furthermore, in proportion to the distance from the collector the gain must drop at the relaxation rate of molecules at the upper laser level.

Thus, for the absolute value of the gain in the case of a homogeneous mixture with $W/g = 300$ J/g and $[CO_2] = 5$ to 15 percent, we would have $K_0 = 1.5$ to 4.5 %/cm, which is severalfold higher than the measured value. The drop in gain in relation to the chamber's length for a Teflon collector takes place with $x > 4$ cm and CO_2 concentrations of 7.5 to 12 percent with effective times within the range of 0.2 to 0.3 ms. For the purpose of comparison let us use the data on vibrational relaxation coefficients from survey [6]. For these we have (in units of (mm Hg·s)$^{-1}$):

$$(p\tau)^{-1}_{CO_2-CO_2} = 350; \quad (p\tau)^{-1}_{CO_2-N_2} = 106; \quad (p\tau)^{-1}_{CO_2-H_2O} = 3 \cdot 10^4; \quad (p\tau)^{-1}_{N_2-H_2O} = 35.$$

Comparison of these coefficients speaks in favor of the fact that the major channel for the relaxation of vibrational energy is CO_2-H_2O collisions. The characteristic relaxation time in the case of a homogeneous medium with our composition would equal $\tau_x = 0.2$ to 0.6 ms, which is close to that measured experimentally.

The investigations made make it possible to draw a number of conclusions regarding difficulties in the creation of and operating features of a fast-flow steady-state laser utilizing air and mixing of CO_2 beyond the discharge zone. The experiment has demonstrated that it is possible to create an effectively operating discharge chamber with an efficiency of 0.7 and air pressure of up to $p = 100$ mm Hg and flow rates of approximately 200 m/s.

For the specific electrode system design the unit discharge power equaled $E \sim 70$ W/cm^3, which with a discharge zone length of 2 to 25 cm makes it possible to contribute up to 300 to 400 J/g. As compared with known designs of electrode systems with tubular (cf., e.g., [9,10]) or plate-type [7] cathode elements, the employment of pins protruding into the gas stream makes it possible to increase severalfold the effective pressure of the molecular gas (cf. [9,10]) and the specific bulk power of the discharge and to reduce considerably losses of vibrational energy on account of relaxation in the discharge chamber (cf. [7]). The pin design of the cathode is simple to make and, as demonstrated experimentally, does not require special cooling in operation.

As far as the problem of supplying CO_2 beyond the discharge zone and subsequent mixing of it with the active medium is concerned, it has been shown experimentally that although it is apparently not possible to achieve homogeneous mixing of CO_2 at the molecular level, the value of the gain is totally sufficient for effective operation of the cavity. With a mean relative CO_2 concentration of about 10 percent, the value of the gain equals $K_0 \sim 1$ %/cm. The absolute value of the gain would correspond in a homogeneous mixture to a lower CO_2 concentration, and the rate of the drop in gain on account of the relaxation of vibrational energy has been proven to be close to that expected in the case of a mixture of homogeneous composition.

Thus, based on the experiments conducted it is possible to conclude that the CO_2 laser system discussed is promising.

We wish to express our thanks to Ye.P. Velikhov for initiation of this study and A.A. Vedenov for the interest he has shown.

Bibliography

1. Hill, A.E. APPL. PHYS. LETTS., 18, 194 (1971).

2. Bullis, R.H., Nigan, W.L., Fowler, M.C. and Wiegand, W.J. AIAA J., 10, 407 (1972).

3. Kovsh, I.B. ZARUBEZHNAYA RADIOELEKTRONIKA, No 3, 86 (1973).

4. Tiffany, W.B., Targ, R. and Foster, J.D. APPL. PHYS. LETTS., 15, 91 (1969).

5. Vedenov, A.A. et al. TVT, 14, 441 (1976).

6. Taylor, L. and Bitterman, S. REV. MOD. PHYS., 41, 26 (1969).

7. Artamanov, A.V. et al. KVANTOVAYA ELEKTRONIKA, 4, 581 (1977).

8. Devir, A.D. and Oppenheim, U.P. APPL. OPTICS, 8, 2121 (1969).

9. Ben-Josef, N. et al. J. PHYS., 4, 708 (1971).

CSO: 1862
8831

LASERS AND MASERS

UDC 621.378.33

ANALYTICAL THEORY OF PULSED LASING OF A CO LASER WITH LINE SELECTION

Moscow KVANTOVAYA ELEKTRONIKA in Russian Vol 6 No 9, Sep 79 pp 1966-1970
manuscript received 22 Jan 79

[Article by S.A. Zhdanok, A.P. Napartovich and A.N. Starostin, Institute of Atomic Energy imeni I.V. Kurchatov, Moscow]

[Text] An analytical theory is constructed for the non-steady-state lasing of a CO laser with line selection and a comparison is made with a precise numerical calculation. Equations are given for key characteristics of the lasing pulse, such as maximum power, lasing efficiency, delay time and pulse duration. Also discussed is the establishment of generation when the pump is turned on.

As we know, the lasing spectrum of a CO laser contains a great number of vibrational-rotational transitions of the CO molecule. However, in an entire series of applications, such as isotope splitting, laser spectroscopy, and laser chemistry, it is necessary to have radiation at only a certain single transition. In this connection the investigation of lasing of a CO laser with the selection of different lines is important. In [1] an analytical theory was constructed for a steady-state CO laser with a selective cavity, in which simple expressions were obtained for the generation characteristics of these systems. In this paper an analytical theory is constructed for non-steady-state generation of a CO laser with line selection, and a comparison is made with precise numerical calculations made in [2].

The system of kinetic equations describing the generation of radiation in a selective cavity at the $(m + 1; j) \rightarrow (m; j + 1)$ transition of the CO molecule, where m and j are the vibrational and rotational quantum numbers, has the form

$$df_v/dt=\Pi_{v+1}-\Pi_v+i_v,\quad v=0, 1, 2, \ldots, \tag{1}$$

$$dI/dt=c(k-\Delta)I, \tag{2}$$

where f_v is the percentage of CO molecules in the v-th excited state; Π_{v+1} is the flow of vibrational populations in the space of vibrational

numbers in the cross section between the v-th and (v + 1)-th levels; i_v is the frequency of excitation of the v-th level by external sources; I, k and Δ are the radiation intensity, the gain and losses in the transition considered; and c is the speed of light. In the approximation for single-quantum VV exchange, the expression for Π_{v+1} has the form in [1,3-5]:

$$\Pi_{v+1}=\sum_{v'}\left(Q^{v',\,v'+1}_{v+1,\,v}f_{v+1}f_{v'}-Q^{v'+1,\,v'}_{v,\,v+1}f_{v}f_{v'+1}\right)+\left(P_{v+1}+A_{v+1}\right)f_{v+1}+$$
$$+\frac{I\sigma}{\hbar\omega}\left(f_{v+1}-\delta f_v\right)\delta_{v,\,m},\qquad(3)$$

where $\overline{Q}^{v',v'+1}_{v+1,v}$, A_v and P_v are the frequencies of VV exchange, spontaneous disintegration and relaxation from the v-th level (thermal excitation from the v-th level is unlikely); $\sigma \sim (m + 1) \exp[-Bj^2/(T)]$ is the effective cross section of induced radiation at the $(m + 1) \to m$ transition at frequency ω; $\delta = \exp(-2Bj/T)$; B is the rotational constant; $\delta_{v,m}$ is the Kronecker symbol; and T is the temperature of the gas. Below we will be interested in the case when an external source excites only lower vibrational levels and the generation of radiation takes place only at frequencies where VT losses and spontaneous radiation can be disregarded. Then, proceeding to continuous variable v and using the approximation of resonance VV exchange in [1,3-5], system (1) can be approximately substituted by the equation

$$\frac{\partial f_v}{\partial t}=\nu\frac{\partial^2}{\partial v^2}\left[(v+1)^2f_v^2\right]+\frac{\partial}{\partial v}\left[\frac{I\sigma}{\hbar\omega}\left(\frac{\partial f_v}{\partial v}+\gamma f_v\right)\delta(v-m)\right],$$
$$\nu=\frac{2\Delta E}{T}\int_0^\infty Q^{v',\,v'+1}_{v+1,\,v}\frac{(v-v')^2}{(v+1)(v'+1)}\,dv'\sim N_{CO}(T),\qquad(4)$$

where $\delta(x)$ is the Dirac delta function; $\gamma = 1 - \delta$; ΔE is the energy of anharmonicity; and N_{CO} is the density of CO molecules. As is obvious from equation (4), f_v changes at characteristic times on the order of ν^{-1}. The establishment of intensity takes place after a cavity period on the order of $(c\Delta)^{-1}$. As a rule, $\nu \ll c\Delta$, which makes it possible to employ an approximation of quasi-steady-state generation:

$$\sigma(f_{m+1}-\delta f_m)=\Delta/N_{CO}.\qquad(5)$$

Now substituting (5) in (4) and integrating (4) in the vicinity of point m it is easy to get

$$I\Delta=\nu\hbar\omega(m+1)^2(f_m^2-f_{m+1}^2)N_{CO}.\qquad(6)$$

Since the value of f_m is found from (4) (with $I = 0$), and of f_{m+1} from (5), then the problem posed has in principle been solved. Let us note that the value of distribution function f_v in region $v \leq m$ does not depend on the existence of generation and is determined only by excitation conditions. The time for the start and termination of generation can be found from (6) by having equated the radiation intensity to zero, i.e., by having solved in terms of t the equation

$$f_m(t) = f_{m+1}(t). \tag{7}$$

It follows from (5) and (7) that the time for the start and termination of generation corresponds to moments at which at level m is reached a threshold population of $f_m = \Delta(\sigma\gamma N_{CO})^{-1}$. The threshold characteristics (energy contribution and pumping power) are now defined as the values of the corresponding parameters with which for the first time a solution is found for equation (7). Let us dwell in greater detail on the problem of computing $f_m(t)$. Equation (4), for $v \leq m$, by substitution of variable $\tau = \int_0^t \nu\, dt$ is reduced to the form

$$\frac{\partial f_v}{\partial \tau} = \frac{\partial^2}{\partial v^2}\left[(v+1)^2 f_v^2\right], \tag{8}$$

which makes it possible to take into account the change in ν over time, caused, e.g., by heating of the gas. Of greatest interest are the cases of generation with pulsed excitation and when steady pumping is switched on. As demonstrated in [6,7], it is precisely in these cases that it is possible to find fairly simple solutions to equation (8). In particular, for pulsed excitation with an energy contribution density of ε, when for a single molecule are necessary $n = \varepsilon(N_{CO}\hbar\omega)^{-1}$ vibrational quanta, in [7] the following solution is gotten to equation (8):

$$f_v(t) = \left(\frac{3}{4}n\right)^{1/4} \frac{1}{\sqrt{v+1}\,\tau^{3/4}} - \frac{1}{2\tau}. \tag{9}$$

Equation (9) describes the propagation in space of vibrational numbers of the excitation "wave," which was originally localized in the area of low v. By its means are easily found the following parameters characterizing the process of determination of the distribution function for vibrational numbers: time τ_m for the arrival of the excitation "wave" at point m, and time τ_M for achieving maximum population density at level m, and its value, f_M:

$$\tau_m = (m+1)^2/(12\,n);\quad \tau_M = (4/3)^4\tau_m;\quad f_M = (6\tau_M)^{-1}. \tag{10}$$

From condition (7) it is possible to obtain the following expression for the time for the beginning, τ_0, and end, τ_1, of generation:

$$\tau_{0,1}=\left(-{}^1/_2\sqrt{y}\pm\sqrt{A/(2B\sqrt{y})-{}^1/_4y}\right)^4;$$
$$y=\alpha_1+\alpha_2;\quad \alpha_{1,2}=\left[\frac{A^2}{2B^2}\pm\sqrt{\left(\frac{A^2}{2B^2}\right)^2-\left(\frac{2}{3B}\right)^3}\right]^{1/3};$$
$$A=({}^3/_4n)^{1/2}/\sqrt{m+1};\quad B=\Delta(\sigma\gamma N_{CO})^{-1}. \tag{11}$$

If the threshold value of $\tilde{f}_m$ is much lower than the maximum population density of level m determined by equation (10), i.e., the condition is fulfilled of

$$\Delta/(\sigma\gamma N_{CO})\ll n/(m+1)^2, \tag{12}$$

then the time for the start of generation practically coincides with the time for the arrival of the excitation "wave" at point m. The equation for the time for the termination of generation is also simplified in this case:

$$\tau_1\approx(\sigma N_{CO}\,\gamma/\Delta)^{1/4}\,[{}^3/_4n(m+1)^{-2}]^{1/2}. \tag{13}$$

Obviously, corresponding to the threshold case are those values of parameters when the maximum population density of level m agrees with the threshold:

$$f_M=\Delta/(\sigma\gamma N_{CO}). \tag{14}$$

Utilizing (10), from (14) we find the threshold reserve of quanta and the threshold time for the start of generation, τ:

$$\frac{3}{4}\tilde{n}=\frac{32}{27}\frac{\Delta}{\sigma\gamma N_{CO}}(m+1)^2,\quad \tilde{\tau}=\frac{1}{6}\frac{\sigma\gamma N_{CO}}{\Delta}. \tag{15}$$

Since $\sigma\sim(m+1)$, then from (15) it follows that

$$\tilde{n}\sim\frac{(m+1)\,\Delta}{N_{CO}}\frac{\exp[Bj^2/(T)]}{1-\exp(-2Bj/T)},\quad \tilde{n}\tilde{\tau}\sim(m+1)^2. \tag{16}$$

In fig 1 is made a comparison of $I(t)$ curves, one of which has been calculated by equation (6) with ν = const, and the second was obtained by a numerical solution to system (1), (2), taking into account heating of the gas [2]. The agreement is obviously fairly convincing. Let us note that

disregarding heating of the gas is valid in describing only the initial stage of generation. Taking into account heating of the gas, as already mentioned, reduces to replacing in all equations magnitude νt by $\int_0^t \nu\, dt$, which with a known $T(t)$ dependence complicates the problem insignificantly.

As is obvious from (6) the intensity of radiation reaches a maximum value of I_M at moment of time τ_M, whereby

$$I_M \Delta = N_{CO} \nu \hbar \omega (m+1)^2 \left[f_M^2 \gamma (2-\gamma) - \frac{2\Delta}{\sigma N_{CO}} (1-\gamma) f_M - \frac{\Delta^2}{\sigma^2 N_{CO}^2} \right]. \tag{17}$$

From (17) it is easy to find that near the generation threshold $I_M \sim (n - \bar{n})(m+1)^2$, and when the threshold is exceeded considerably, $I_M \sim \varepsilon^2 (m+1)^{-2} \Delta^{-1} N_{CO}^{-1} [1 - \exp(-4Bj/T)]$. For the efficiency of selective generation, in disregarding heating of the gas, it is possible to obtain the following equation:

$$\eta = \eta_v \frac{\nu \hbar \omega}{n E_1} (m+1)^2 [F(t_1) - F(t_2)], \tag{18}$$

where E_1 is the energy of the lower vibrational quantum; η_v is the percentage of energy going toward the excitation of vibrations; $t_{0,1} = \tau_{0,1} \nu^{-1}$;

$$F(t) = \frac{\Delta}{\sigma N_{CO} \nu} (1-\gamma) \ln t - \frac{\gamma(2-\gamma)}{12 \nu^2 t} - \frac{3\Delta^2 t}{\sigma^2 N_{CO}^2 \gamma} (4-3\gamma). \tag{19}$$

Under over-the-threshold conditions from (18) and (19) it is easy to get

$$\eta \approx \eta_v N_{CO} \hbar \omega \varepsilon^{-1} \gamma (2-\gamma) \sim [1 - \exp(-4Bj/T)]. \tag{20}$$

As is obvious from (20), with high energy contributions (with condition (12)), the efficiency of selective generation tends toward a constant value slightly dependent on the number of the vibrational level, m (only in terms of ω and γ) and on losses, Δ. Near the generation threshold (18) takes the form

$$\eta \approx 16 \left(\frac{2}{3}\right)^{4/3} \eta_v \frac{\hbar \omega \Delta}{\varepsilon \sigma} (10 - 7\gamma) \left(\frac{n}{\bar{n}} - 1\right)^{4/3}. \tag{21}$$

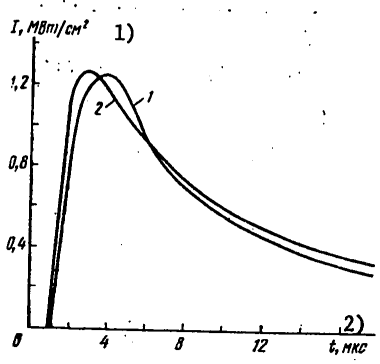

Figure 1. I(t) Curves with Pulsed Excitation, Obtained in [2]$_3$(1) and from Calculation by Equation (6) (2): $\varepsilon = 0.05$ J/cm^3; mixture of CO:Ar = 1:10; p = 100 mm Hg; T = 80°K; $\Delta = 10^{-3}$ cm^{-1}; m = 9; j = 13

Key:
1. I, MW/cm^2
2. t, μs

Let us now consider selective generation in the case when in the system a steady pumping source with power W (in terms of a single molecule) is turned on and off. Then, as demonstrated in [6,7], distribution function f_v in region $v \leq m$ is determined by the equation

$$f_v = C/(v+1) - 1/(2\tau) \tag{22}$$

for the case of turning the source on, and

$$f_v = \begin{cases} \frac{C}{v+1}\left[1-\exp\left(-\frac{v+1}{2\tau C}\right)\right], & \tau \ll \frac{v+1}{2C}, \\ \sqrt{\frac{C}{\tau(v+1)}}, & \tau \gg \frac{v+1}{2C} \end{cases} \tag{23}$$

for the case of turning the source off, where $C = \sqrt{W\eta_v/(E_1\nu)}$. Substituting (22) and (23) with $v = m$ in (6), it is possible to obtain the dependence I(t). Solving (7) with f_m from (22), we obtain the following expression for the time, τ_0, for the delay of generation when the source is turned on:

$$\tau_0 = \frac{1}{2}\left(\frac{C}{m+1} - \frac{\Delta}{\sigma\gamma N_{CO}}\right)^{-1}. \tag{24}$$

The threshold pumping power, $\tilde{W}$, can be obtained from (24), with τ_0 tending toward infinity:

$$\tilde{W} = \nu\left(\frac{\Delta}{\sigma\gamma N_{CO}}\right)^2 (m+1)^2 \frac{E_1}{\eta_0} \sim \frac{\Delta^2 \exp(Bj^2/T)}{[1-\exp(-2Bj/T)]^2} N_{CO}^{-2}. \tag{25}$$

In the case when the threshold is exceeded considerably, when the condition

$$C \gg \Delta(m+1)/(\sigma\gamma N_{CO}), \tag{26}$$

is fulfilled, the time for the delay of generation agrees with the time, τ_m, for the arrival of the excitation "wave" at point m:

$$\tau_m = (m+1)/(2C). \tag{27}$$

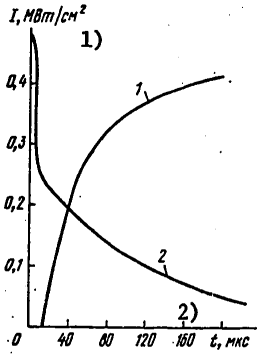

Figure 2. I(t) Curve Plotted from Equation (6) for Turning the Source On (1) and Off (2); $W = 714$ W/cm^3; remaining parameters the same as in fig 1

Key:
1. I, MW/cm^2
2. t, μs

In fig 2 as an example is given the result of calculating the radiation intensity, I(t), from equation (6) for the case of turning the source on and off and disregarding heating of the gas.

In conclusion let us note that the equations which we have obtained can describe selective generation also with other diatomic molecules of the HCl, HF, etc., type, and are also easily generalized for the case of selective generation with overtones of diatomic molecules.

Bibliography

1. Napartovich, A.P., Novobrantsev, I.V. and Starostin, A.N. KVANTOVAYA ELEKTRONIKA, 4, 2125 (1977).

2. Konev, Yu.B., Kochetov, I.V. and Pevgov, V.G. "Tezisy dokladov II Vsesoyuznogo seminara po fizicheskim protsessam v gazovykh OKG" [Theses of Papers at the Second All-Union Seminar on Physical Processes in Gas Lasers], Uzhgorod, 1978, p 58.

3. Brau, C.A. PHYSICA, 86, 533 (1972).

4. Gordiyets, B.F., Mamedov, Sh.S. and Shelepin, L.A. Preprint FIAN, 1974, No 28.

5. Gordiyets, B.F. and Mamedov, Sh.S. ZHURN. PRIKL. TEKH. I TEKHN. FIZ., No 3, 13 (1974).

6. Zhdanok, S.A., Napartovich, A.P. and Starostin, A.N. "Tezisy dokladov II Vsesoyuznogo seminara po fizicheskim protsessam v gazovykh OKG," Uzhgorod, 1978, p 46.

7. Zhdanok, S.A., Napartovich, A.P. and Starostin, A.N. ZHETF, 76, No 1 (1979).

CSO: 1862
8831

LASERS AND MASERS

UDC 621.373.826

EFFICIENCY OF EXIMER LASERS UTILIZING MOLECULES OF HALIDES OF NOBLE GASES EXCITED BY AN ELECTRON BEAM

Moscow KVANTOVAYA ELEKTRONIKA in Russian Vol 6 No 9, Sep 79 pp 2024-2027
manuscript received 12 Jul 78

[Article by V.V. Ryzhov and A.G. Yastremski, USSR Academy of Sciences Siberian Division Institute of High-Current Electronics, Tomsk]

[Text] By means of solving equations for the kinetics of processes in the plasma of eximer lasers utilizing molecules of halides of noble gases, equations are obtained which make it possible to estimate the efficiency of such lasers excited by an electron beam. The numerical modeling of processes in eximer lasers has demonstrated that the equations obtained can be used for calculating efficiency with a gas pressure from 1 to 10 atm. The results are give of calculations of the limiting efficiency of lasers utilizing molecules of KrF*, XeCl* and XeBr*.

The method of exciting gases with an electron beam is one of the promising methods of pumping high-power gas lasers generating radiation in the short wavelength region. One of the main problems of the theory of these lasers is the determination of the efficiency, η , of the conversion of the beam energy absorbed in the gas into stimulated radiation. Usually for the purpose of estimating the maximum efficiency of a laser is utilized the quantum efficiency, equal to the ratio of the energy of a laser photon, $h\nu$, to the potential for the formation of active particles of plasma, I , whose energy as the result of a series of elementary processes can be transferred to the upper laser level: $\eta_{max} \leq \eta_{kv}$, $\eta_{kv} = h\nu/I$.

It is well known that such estimates are quite approximate and for some systems can exceed the real efficiency of a laser by more than an order of magnitude. In this paper equations are obtained which make it possible to refine, as compared with η_{kv} , the estimate of the maximum efficiency of lasers utilizing halides of noble gases excited by an electron beam, because of taking into account the effectiveness of the input of beam energy into the gas and the kinetics of processes in the plasma.

Let, in the working space of a laser, per unit of time, a beam form N active particles, expending on this a portion of the absorbed energy, ξ ,

and let each active particle as the result of a chain of reactions be able to result in pumping of the upper laser level. If then the laser emits n photons, then the efficiency of this laser in the steady-state mode is determined by the equation

$$\eta = \xi(n/N)(h\nu/I) = \xi\gamma\eta_{KB}. \tag{1}$$

Here factor $\gamma = n/N$ characterizes the effectiveness of the transfer of excitation through the reaction chain to the working level; it is equal to the mean number of laser photons required for one active particle formed by the electron beam in the working space of the laser.

Equation (1) determines the effectiveness of a laser in the case when pumping of the upper level takes place through a single channel. From this viewpoint the kinetics of processes in the plasma of eximer lasers utilizing halides of noble gases are fairly complex. An analysis has shown [1-3] that in the case when the buffer gas is argon, the working molecule RX* (R is an atom of xenon or krypton and X is a halogen atom) is formed through several channels. Thus, the energy expended by the beam for the ionization of atoms of argon is transmitted, via conversion processes and resonance charge transfer, to elemental ions R^+. In addition, R^+ ions can be formed directly by the beam. Eximeric molecules of RX* are formed in these two reaction chains as the result of the process of ion-ion recombination. This channel for the formation of RX* we will call the ionic channel.

The energy spent by the beam for the excitation of atoms of argon is transmitted via processes of resonance excitation transfer and conversion to metastable levels of R* atoms. These levels in addition can be excited by the beam directly. Molecules of RX* are formed in this channel, which we will call the excitation channel, as the result of the reaction of R* with a halogen carrier.

The kinetic link between channels is accomplished via processes of electron recombination, as the result of which metastable states of Ar* and R* are formed. In certain cases these processes can be disregarded by comparison with the more rapid reactions of ion-ion recombination. In such a model the link between channels is broken, and the formation of RX* can be considered independent for both channels, which considerably simplifies the calculation of efficiency.

As follows from the system employed, the beam energy is transmitted into each channel in two ways: via ionization or excitation of atoms of the buffer gas and atoms of krypton or xenon. Therefore it must be expected that the total efficiency of a laser utilizing halides of noble gases will be equal to the sum of the efficiencies of each energy transfer channel. Actually, solving kinetics equations for the steady-state case in an approximation for independent channels, it is possible to obtain an expression for efficiency in the form

$$\eta=\eta^{l}+\eta^{*},$$
$$\eta^{l}=\xi^{l}_{Ar}\gamma^{l}_{Ar}\eta^{l}_{Ar}+\xi^{l}_{R}\gamma^{l}_{R}\eta^{l}_{R},\quad \eta^{l}_{B}=h\nu/I^{l}_{B},$$
$$\eta^{*}=\xi^{*}_{Ar}\gamma^{*}_{Ar}\eta^{*}_{Ar}+\xi^{*}_{R}\gamma^{*}_{R}\eta^{*}_{R},\quad \eta^{*}_{B}=h\nu/I^{*}_{B}, \tag{2}$$

where $\eta^{*(i)}$ is the efficiency of the excitation channel (or ionic channel); $\gamma^{*(i)}_{B}$ is the mean number of laser photons formed as the result of transfer of the beam energy toward the excitation of metastable states of B^{*} atoms (or for the formation of B^{+} ions) calculated for a single active particle; and $\eta^{*}_{B}(i)$ is the quantum efficiency of the respective energy transfer channels.

If one disregards the process of collision disintegration of eximeric molecules of RX* by equating with the process of induced radiation, then for $\gamma^{*(i)}_{B}$ the following fairly simple equations can be obtained:

$$\gamma^{l}_{R}=G^{-1},$$
$$\gamma^{l}_{Ar}=\gamma^{l}_{R}C^{2}\alpha_{1}\alpha_{2}[Ar]^{2}[R]/(1+\alpha_{1}C[Ar]^{2})(1+\alpha_{2}C[R]),$$
$$\gamma^{*}_{R}=(1+\beta_{2}[Ar][R]/\alpha_{e2}[X_{n}])^{-1},$$
$$\gamma^{*}_{Ar}=\gamma^{*}_{R}/(1+\alpha_{e1}[X_{n}]/\beta_{1}[Ar]^{2}, \tag{3}$$

where $\alpha_{1,2}$ are the constants for the conversion of elemental ions of argon into molecular and for charge transfer from Ar^{+}_{2} to R; $\beta_{1,2}$ are the conversion constants for Ar* into Ar^{*}_{2} and R* into R^{*}_{2}, respectively; and $\alpha_{e1,e2}$ are the constants for the reaction of Ar* and R* with halogen carrier X_{n}.

Let us note that the values of coefficients $\gamma^{*(i)}_{B}$ depend on the model used for processes in the active medium of the laser. Thus, if we use as a basis the model of processes suggested in [1], but assume that in the recombination of Ar^{*}_{2} and R^{*}_{2} ions molecules of ArX* and RX* are formed (model 1), then $G = 1$. And if it is assumed that as the result of this reaction are formed the complexes $Ar_{2}X^{*}$ and $R_{2}X^{*}$ (model 2), then

$$G=(1+\alpha_{3}C[Ar][R]),$$

where α_{3} is the conversion constant for R^{+} into R^{+}_{2}.

Coefficient C included in the expression for γ^{i}_{Ar} and G is equal to the ratio of the total concentration of positive ions in the plasma, $[P^{+}]$, to the rate of formation of electrons by the beam, ψ_{e}:

$$C=[P^{+}]/\psi_{e}. \tag{4}$$

In the steady-state case

$$[P^+] = \psi_e[(\alpha_{pr}[X_n] + (1 + 4\alpha_{np}^2[X_n]^2/\alpha_r\alpha_p)^{1/2}]/2\alpha_{np}[X_n], \quad (5)$$

where α_{pr} is the constant for the adhesion of electrons to the halogen carrier and α_r is the ion recombination constant. Values of ψ_e can be computed by the equation

$$\psi_e = jD/e\varepsilon_i. \quad (6)$$

Here j is the current density of the beam; e is the charge of the electrons; ε_i is the energy for the formation of an electron-ion pair, whose values for mixtures of noble gases are given in [4]; and D is the amount of energy absorbed per unit volume of gas, calculated for a single beam electron, taking into account processes of the scattering of electrons and the absorption of energy in the foil [5].

For calculations by equation (2) it is necessary to know the percentage of energy spent by the beam for the ionization of atoms of argon, ξ_{Ar}^i, and xenon (or krypton), ξ_R^i, as well as the energy which went to the formation of metastable and resonance levels of these atoms, ξ_{Ar}^* and ξ_R^*. We calculated the values of these magnitudes for mixtures of Ar-Kr and Ar-Xe by modeling the exchange of electron energy by the Monte Carlo method [6]. This method makes it possible to make a detailed analysis of expenditures of beam energy for the formation of atoms and ions in different excited states. An analysis of the results of calculation of the distribution of the energy of an electron beam in mixtures of Ar-Kr and Ar-Xe, given in table 1, show that for a mixture in which the relative concentration of the second component is less than 0.1, the main share of the beam energy (approximately 50 percent) goes toward the ionization of argon, whereas for the formation of R^+ ions five- to 10-fold less energy is spent. Approximately 25 percent of the energy in these mixtures goes toward the excitation of atoms of argon, whereby almost a third of it goes to the formation of atoms of argon in metastable and resonance states, Ar*(m + r), and just as much for the formation of atoms of argon, Ar*(p), in p states. It is interesting to note that for the excitation of R atoms is used just as much energy as for the ionization of these atoms, whereby the beam mainly forms atoms of Kr* or Xe* in metastable or resonance states, R*(m + r). As demonstrated in [6], this fact is explained by the fact that the cross sections for the excitation of these levels by an electron beam are not screened by the cross sections of argon.

Let us note that the potentials for the excitation of the lower electronic states of atoms of noble gases, I^*, are high; therefore a considerable portion of the energy ($q \sim 20$ percent) in mixtures of noble gases is transferred to subthreshold electrons whose energy is lower than I^*. In laser mixtures the energy of these electrons is transferred to molecules of the halogen carrier and is lost in elastic collisions with atoms of the noble gas. Calculations made for three-component mixtures have shown that in connection

with the low concentration of molecules of the halogen carrier in laser mixtures the addition of it to a mixture of noble gases practically does not change expenditures of the beam's energy for the ionization and excitation of atoms of Ar and R. Therefore for approximate estimates of the efficiency of lasers employing halides of noble gases it is possible to use the results of calculations of $\xi_R^{*(1)}$ obtained for mixtures of noble gases.

For the purpose of revealing the area of applicability of the equations obtained, a program was written for the numerical solution of the kinetics equations suggested in [1], together with equations for the flow of laser photons. In the program were taken into account processes of the collision and spontaneous disintegration of eximer molecules and the absorption of laser photons in the active medium, as well as processes of electron-ion recombination, which were not taken into account in deriving equations (2) to (5). Calculations were made for an XeCl laser utilizing a mixture of Ar-Xe-CCl_4 excited by an electron beam. The results of calculations of the power of laser radiation agreed with those experimentally observed in [4], and the real efficiency of a laser excited by a beam of 50 ns duration equaled three to four percent.

In fig 1 are given the results of calculation of the efficiency of the steady-state operating mode of an XeCl laser. Efficiency was defined as the ratio of the power of laser radiation in the steady-state region of the laser's operation to the power of the electron beam entering the gas. Comparison of these results with the results of calculations by equations (2) to (5) shows that the expressions obtained are of an approximate nature and can be used only for estimating the maximum efficiency of lasers utilizing halides of noble gases. Furthermore, as would be expected, the equations obtained in model 1 give an upper estimate of the efficiency of these lasers, while model 2 with sufficiently high pressures can prove to be unacceptable for such estimates. Analysis of the results of calculations by these equations showed that the main contribution to the laser's radiation is made by the ionic channel (as much as 80 percent in model 1). The low contribution of the excitation channel is caused by two facts: First, the percentage of the energy which goes toward the formation of atoms of noble gases in metastable and resonance states is not greater than 10 to 15 percent (cf. table 1), and secondly the efficiency of the transfer of energy to the excitation channel is low (e.g., $\gamma_{Ar}^* = 0.1$ to 0.5). Let us note that the conclusion regarding the decisive role of the ionic channel in the formation of eximer molecules in excitation with an electron beam has been confirmed experimentally [2,4]. Taking into account the fact that the ionic channel makes the main contribution to the formation of eximer molecules, approximate estimates of efficiency can be made without taking into account the contribution of the excitation channel, $\eta \simeq \eta^i$.

Let us note that in model 1 $\gamma_R^i = 1$ and the values of γ_{Ar}^i , as indicated by calculations, are also fairly high and depending on the concentration of R atoms and the pressure of the gas vary from 0,6 to 0.9. Therefore, for rough estimates of the upper limit of efficiency it is possible to assume that $\gamma_{Ar}^i \simeq \gamma_R^i = 1$ and to use the equation

$$\eta_{max} \leqslant \xi^{i}_{Ar}\eta^{i}_{Ar} + \xi^{i}_{R}\eta^{i}_{R}. \quad (7)$$

With low concentrations (less than 10 percent) of Kr or Xe atoms in argon the second term in this formula can be disregarded and a fairly simple formula can be obtained for estimating the efficiency of lasers utilizing halides of noble gases [4]:

$$\eta \leqslant \xi^{i}_{Ar}\eta^{i}_{Ar}. \quad (8)$$

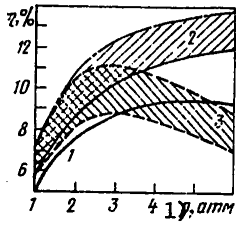

Figure 1. Dependence of Efficiency of an XeCl Laser on Pressure of the Mixture Ar:Xe:CCl_4 = 1600:40:2 with j = 28 A/cm^2 Curve 1--results of modeling on a computer according to the model in [1]: bands 2 and 3--calculation by equations (2) to (5) in model 1 and 2, respectively; contribution of excitation channel indicated by hatching

Key:
1. p , atm

Table 1.

Состав смеси 1) / ξ	Ar^+	Ar^*	$Ar^*(m+r)$	$Ar'(p)$	R^+	R^*	$R^*(m+r)$	q
Ar	0,571	0,239	0,079	0,079	—	—	—	0,19
0,9Ar -- 0,1Xe	0,438	0,240	0,064	0,078	0,07	0,071	0,068	0,181
0,97Ar — 0,03Xe	0,494	0,264	0,075	0,098	0,023	0,024	0,023	0,20
0,9Ar -- 0,1Kr	0,464	0,250	0,071	0,093	0,063	0,030	0,026	0,193
0,99Ar — 0,01Kr	0,517	0,284	0,080	0,11	0,0067	0,0036	0,0028	0,19

[Key on following page]

Key:
1. Composition of Mixture

Table 2.

1) Молекула эксимера	2) $\eta_{кв}$	η_{max}	η_1	f_{η_1}	η_2	f_{η_2}	3) $\eta_{эксп}$	j, А/см²	p, атм	4) Состав смеси	5) Литература
KrF*	0,32	0,16	0,14	0,13	0,12	0,11	0,09	11,5	1,7	Ar:Kr:F_2 = = 95,8:4:0,2	[2]
XeCl*	0,26	0,13	0,12	0,11	0,09	0,08	0,026	75	5	Ar:Xe:CCl_4 = = 3200:100:1	[4]
XeBr*	0,28	0,15	0,12	0,11	0,11	0,09	0,005	125	5	Ar:Xe:$C_2F_4Br_2$ = = 2000:40:1	[7]

Key:
1. Molecule of eximer
2. η_{kv}
3. η_{eksp} [experimental]
4. Composition of mixture
5. Bibliography

In table 2 values of the efficiency of different lasers utilizing halides of noble gases, calculated by equations (2) to (5) in model 1 (η_1) and in model 2 (η_2), are compared with the quantum efficiency of these systems, η_{kv}, which is often used for estimating maximum efficiency. Given here also is the contribution to efficiency of the ionic channel in model 1 (η_1^1) and in model 2 (η_2^1). The calculations were made for the conditions of the experimental studies referred to in the table. It follows from table 2 that calculation by equations (2) to (5) lowers more than twofold the upper limit of efficiency, as compared with the quantum efficiency. Thus, for lasers utilizing molecules of KrF* the maximum efficiency realized experimentally equaled nine percent. whereas the estimate by the equations gives 14 percent. This estimate is closer to the real efficiency than η_{kv} (32 percent).

Bibliography

1. Rokni, M., Jakob, J.H., Mangano, J.A. and Brochu, R. APPL. PHYS. LETTS., 31, 79 (1977).

2. Rokni, M., Mangano, J.A., Jacob, J.H. and Hgia, J.C. IEEE J., QE-14, 464 (1978).

3. Basov, N.G., Danilychev, V.A., Dolgikh, V.A., Kerimov, O.M. and Molchanov, A.G. "Tezisy dokladov II Vsesoyuznogo seminara po fizicheskim protsessam v gazovykh OKG" [Theses of Papers at the Second All-Union Seminar on Physical Processes in Gas Lasers], Uzhgorod, 15-17 May 1978, p 101.

4. Bychkov, Yu.I., Konovalov, I.N., Losev, V.F., Mesyats, G.A., Ryzhov, V.V., Tarasenko, V.F., Shemyakina, S.B. and Yastremskiy, A.G. IZV. AN SSSR, SER. FIZICHESKAYA, 42, 2492 (1978).

5. Yevdokimov, O.B., Ryzhov, V.V. and Yalovets, A.P. ZHTF, 47, 2517 (1977).

6. Ryzhov, V.V. and Yastremski, A.G. IZV. VUZOV SSSR, SER. FIZIKA, No 11, 133 (1978).

7. Konovalov, I.N. and Tarasenko, V.F. KVANTOVAYA ELEKTRONIKA, 6, 400 (1979).

CSO: 1862
8831

LASERS AND MASERS

UDC 621.378.33+539.196.5

PERIODIC-PULSE OPERATING MODE OF A QUARTZ-LAMP-PUMPED IODINE ULTRAVIOLET LASER

Moscow KVANTOVAYA ELEKTRONIKA in Russian Vol 6 No 9, Sep 79 pp 2033-2034
manuscript received 20 Apr 79

[Article by V.S. Zuyev, L.D. Mikheyev, A.V. Startsev and A.P. Shirokikh, USSR Academy of Sciences Physics Institute imeni P.N. Lebedev, Moscow]

[Text] A periodic-pulse operating mode has been realized for a laser utilizing molecular iodine (λ = 342 nm) with the employment of quartz lamps as the source of optical pumping. The pulse repetition rate equaled 0.5 Hz and the lasing energy equaled 10 to 50 mJ in a pulse with a pulse duration of 3 to 5 μs at half-height.

Recently we reported on the observation of lasing by employing molecular iodine in the 342 nm region with optical pumping by means of the broadband radiation of an open high-current discharge initiated by the electrical flashing of a fine tungsten wire [1,2]. Up to the present with parameters close to those indicated in [2] we have gotten a lasing energy of approximately 2 J.

For the purpose of implementing the periodic-pulse operating mode for a laser when pumping by means of an open high-current discharge it is necessary to develop methods of periodically initiating the discharge and of replacing the working mixture in the laser chamber after each pulse. In particular, it is possible to use an extended collective radiation source of the open type in [3], comparable in its characteristics with the source we used, and at the same time capable of operating in the periodic-pulse mode. The need to replace the working mixture is caused by the partial or total destruction of the material involved in the discharge plasma.

For the purpose of pumping an iodine laser it is also possible to use pulsed quartz lamps, since the excitation spectrum of iodine vapors lies in the region of 180 to 210 nm. They have less luminance in the ultraviolet region, as compared with an open high-current discharge, but on the other hand they make it possible to operate without replacing the working material. This method of pumping was implemented in this study.

Potential curves for the iodine molecule were calculated in [4]; levels relating to the laser cycle are given in fig 1, employing the designations suggested

in [5]. Pumping takes place from the ground X state. The non-radiative transition between upper levels D and D' is caused by collision with the buffer gas, laser transition $D' \rightarrow A'$ is allowed ($\tau \approx 6$ and 7 ns [6]), and relieving of high ($v'' \approx 14$ and 15) vibrational levels of the A' state, to which the laser transition takes place, is accomplished because of vibrational relaxation and dissociation.

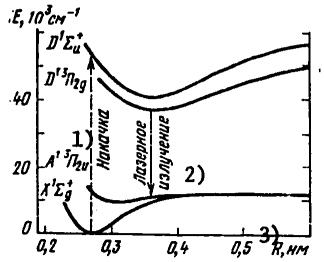

Figure 1.

Key:
1. Pumping
2. Laser emission
3. R , nm

Lasing by utilizing iodine vapors and lamp pumping was observed by us with two laser designs. In one was used an IPKSh lamp 2 cm in diameter and 50 cm long, and in the other a coaxial lamp. The lamps were powered from a 3 μF pulsed capacitor charged to 40 kV. The working mixture consisted of iodine vapors at a pressure of 3 to 5 mm Hg and of perfluomethane at a pressure of 1 to 2 atm. Lasing was observed in both plane and hemispherical cavities with an outlet mirror transmission of two to eight percent. The duration of the lasing pulse equaled 3 to 5 μs at half-height, and its energy, 10 to 50 mJ. The laser operated in the periodic-pulse mode at a frequency of 0.5 Hz. Without replacing the working mixture about 100 flashes were produced, whereby the laser's parameters did not change substantially.

The pulse repetition rate was determined in our experiment by the charging rate of the capacitor. Fundamental restrictions on the pulse repetition rate are imposed first by the recombination time for atoms of iodine formed in the photodissociation of iodine molecules under the effect of radiation in the visible region of the spectrum [7] and secondly by the time for establishing optical homogeneity of the mixture after the pumping pulse. The recombination time for iodine in the working mixture used, according to estimates, equals about 1 μs. Optical inhomogeneities were observed in transilluminating the laser mixture with the beam of an He-Ne laser, and the time for establishing homogeneity of the medium equaled fractions of a second.

Thus, in this study for the first time has been realized a periodic-pulse operating mode for a gas laser with broadband optical pumping by means of a thermal source without replacing the working material. The results obtained testify to the feasibility in principle of creating a sealed-off variant of a laser in the ultraviolet region utilizing iodine vapors.

Bibliography

1. Basov, N.G., Datskevich, I.S., Zuyev, V.S., Mikheyev, L.D., Startsev, A.V. and Shirokikh, A.P. KVANTOVAYA ELEKTRONIKA, 4, 638 (1977).

2. Mikheev, L.D., Shirokikh, A.P., Startsev, A.V. and Zuev, V.S. OPTICS COMMS., 26, 237 (1978).

3. Aleksandrov, V.Ya. and Belosheyev, V.P. ZHPS, 26, 364 (1977).

4. Das, G. and Wahl, A.C. J. CHEM. PHYS., 69, 53 (1978).

5. Tellinghuisen, J. CHEM. PHYS. LETTS., 49, 485 (1977).

6. Sawer, M.C., Jr., Mulac, W.A., Cooper, R. and Grieser, F. J. CHEM. PHYS., 64, 4587 (1978).

7. Kalvert, Dzh. and Pitts, Dzh. "Fotokhimiya" [Photochemistry], Moscow, Mir, 1968.

CSO: 1862
8831

LASERS AND MASERS

UDC 535.375:621.378.325

THEORY OF CAVITIES WITH WAVEFRONT REVERSING MIRRORS

Moscow KVANTOVAYA ELEKTRONIKA in Russian Vol 6 No 9, Sep 79 pp 2036-2038
manuscript received 11 Feb 79

[Article by I.M. Bel'dyugin and Ye.M. Zemskov]

[Text] The problem is discussed of determining the modes of a plane cavity containing as one of the mirrors a wavefront reversing mirror, without restrictions on the dimensions of the mirrors forming the cavity. Expressions are obtained for the fields of modes at the mirrors. It is established that the mode fields of the cavity are in the form of Gauss-Ermite beams with parameters which depend on the ratio of the transverse dimensions of the mirrors.

In connection with the rapid advances in recent times in methods of reversing wavefronts (OVF methods) [1,2], the feasibility has appeared of implementing cavities with OVF mirrors [3,4]. In [3] a report is given on the experimental implementation of a laser with this kind of cavity. In [4] a theoretical study is made of a plane cavity, one of whose mirrors is an OVF mirror and the other an ordinary mirror with infinite transverse dimensions. It is demonstrated that in this kind of cavity the mode fields at the OVF mirror are identical to the fields at the mirrors of a confocal cavity of twice greater length. Furthermore, unlike a confocal cavity, where the type of mode fields is determined chiefly by the curvature of the mirrors and to a lesser extent by diffraction losses in mirrors, in a cavity with an OVF mirror corresponding modes are formed as the result of diffraction losses at the OVF mirror.

For this reason it is possible to expect that generally the kind of mode fields in a cavity with an OVF mirror will depend considerably on the transverse dimensions of both the OVF and the ordinary mirror. In this paper questions are considered, relating to the determination of the modes of a plane cavity containing an OVF mirror, without restrictions on the dimensions of the mirrors forming the cavity.

For the purpose of determining the structure of mode fields of a plane cavity with rectangular mirrors it is sufficient (since the variables in this case have been isolated in [5]) to find a solution to the corresponding unidimensional integral equation. In the case of a plane cavity with an OVF mirror this integral equation has the form:

$$\gamma U(z) = i \int_{-a_2}^{a_2} \int_{-a_1}^{a_1} U^*(x) \exp\{-i\pi[(y-x)^2 + (z-y)^2]\} \frac{U(0)}{U^*(0)} dx dy, \quad (1)$$

where U(x) is the amplitude of the field of the radiation striking the OVF mirror; $a_1 = a_1/(L\lambda)^{1/2}$; $a_2 = a_2/(L\lambda)^{1/2}$; $2a_1$ is the width of the OVF mirror; $2a_2$ is the width of the ordinary plane mirror; L is the distance between mirrors; λ is the wavelength of the radiation; and factor U(0)/U*(0) corresponds to a definite type of OVF mirror and, just as in [4], is introduced in order that the mathematical operation corresponding to the process of reflection of the wave from the OVF mirror will be invariant with regard to the choice for the beginning of the time count.

With $a_2 = \infty$ equation (1) can be integrated in terms of y ; furthermore it is converted to an equation studied in detail in [4]. If $a_2 \neq \infty$, it is not possible to find analytically a solution to equation (1). But in this case information on the kind of solution to equation (1) can be obtained from the equation

$$\gamma U(z) = i \int_{-\infty}^{\infty} \int_{-\infty}^{\infty} U^*(x) \exp[-i\pi[(y-x)^2 + (z-y)^2] - y^2/a_2^2 - x^2/a_1^2] \frac{U(0)}{U^*(0)} dx\, dy, \quad (2)$$

the solutions to which are approximated well by solutions to equation (1) using mirrors with a_1 and a_2 much greater than one. Integrating (2) in terms of y , we get

$$\gamma U(z) = (iB)^{1/2} \int_{-\infty}^{\infty} U^*(x) \exp[-i\pi(x^2 + z^2) - x^2/a_1^2 + i\pi B(x+z)^2] \frac{U(0)}{U^*(0)} dx, \quad (3)$$

$$B = i \frac{\pi a_2^2}{1 + i2\pi a_2^2} = B' + iB''.$$

We will seek a solution to equation (3) by the methods developed in [6]. Let us represent function U(x) in the form

$$U(x) = v(x) \exp(i\pi M x^2), \quad (4)$$

where

$$M = M' + iM''; \quad M' = (B'/\pi a_1^2)/(2B'' + 1/\pi a_1^2); \quad M'' = -1/2\pi a_1^2 + [(2\pi a_1^2)^{-2} + 2M'(B' - 1) + B''/(\pi a_1^2) + 2B' - 1]^{1/2}.$$

Substituting (4) in (3), we get

$$\gamma v(z) = (iB)^{1/2} \sum_{-\infty}^{\infty} v^*(x) \exp\left\{-i\pi A\left(x - \frac{B}{A} z\right)^2\right\} \frac{v(0)}{v^*(0)} dx, \tag{5}$$

where

$$A = M^* - i/(\pi a_1^2) = B + 1.$$

Assuming that a Fourier transform exists,

$$F(\xi) = \frac{1}{\sqrt{2\pi}} \int_{-\infty}^{\infty} f(t) \exp(-i\xi t)\, dt \tag{6}$$

for function $v_x - b\theta$, and, applying it to both halves of equation (5), we get the functional equation

$$\gamma V(\xi) = \left(\frac{A}{B}\right)^{1/2} \frac{v(0)}{v^*(0)} \exp\left[i \frac{A}{4\pi B^2} \xi^2\right] V^*\left(-\frac{A^*}{B^*} \xi\right). \tag{7}$$

All the analytical solutions to (7) are

$$V_n(\xi) = \xi^n \exp\left\{i \frac{A}{4\pi B^2}\left(1 - \frac{|A|^2}{B^{*2}}\right)\left(1 - \left|\frac{A}{B}\right|^4\right)^{-1} \xi^2\right\},$$
$$\gamma_n = (-1)^n \left(\frac{A}{B}\right)^{n+0.5} \frac{v(0)}{v^*(0)}, \quad n = 0, 1, 2, \ldots \tag{8}$$

From (8), taking into account (4), we get

$$U_n(x) \sim H_n(\sqrt{2\alpha}\, x) \exp[-(\alpha + i\beta) x^2], \tag{9}$$

where

$$\alpha = \left\{-\frac{1}{2}\gamma a_1^{-2} + \left[\left(\frac{\gamma a_1^{-2}}{2}\right)^2 + \left(2\pi\gamma - 4\pi^3 a_2^4\right)\beta\gamma + \pi^2\gamma(\Delta - 1) - \beta^2\gamma^2\right]^{1/2}\right\}\gamma^{-1};$$
$$\beta = \frac{2\pi^3 a_2^2 + \pi a_1^{-2} + 2\pi^3 a_2^4 a_1^{-2}}{4\pi^2 a_2^4 a_1^{-2} + a_1^{-2} + 2\pi^2 a_2^2}; \quad \gamma = 1 + (2\pi a_2^2)^2; \quad \Delta = \frac{a_2^2}{a_1^2}. \tag{10}$$

Then assuming that a_1 and a_2 are much greater than one, which as a rule takes place for real mirrors, from (10) it is possible to get

$$\alpha \approx \pi \frac{[(1+\Delta)\Delta]^{1/2}}{1+2\Delta}, \quad \beta \approx \pi \frac{1+\Delta}{1+2\Delta}. \tag{11}$$

Thus, the fields of modes in the cavity considered are in the form of Gauss-Ermite beams. Furthermore the halfwidth and radius of curvature of the beam at the OVF mirror are

$$w = \left(\frac{L\lambda}{\alpha}\right)^{1/2} = \left[\frac{L\lambda(1+2\Delta)}{\pi}\right]^{1/2} [(1+\Delta)\Delta]^{-1/4}, \quad R = \frac{\pi L}{\beta} = L\frac{1+2\Delta}{1+\Delta}, \tag{12}$$

and at the ordinary mirror

$$w_0 = \frac{\alpha/\beta}{[1+(\alpha/\beta)^2]^{1/2}} w = \left(\frac{L\lambda\Delta}{\pi}\right)^{1/2} [(1+\Delta)\Delta]^{-1/4}, \quad R_0 = \infty. \tag{13}$$

Expressions (9) to (13) represent a solution to the problem posed of finding the kind of mode fields of a plane cavity with an OVF mirror. Furthermore, from (9) to (13) with $\Delta = \infty$, in total agreement with the results of [4], it follows that the mode fields at an OVF mirror agree with the fields at mirrors of a confocal cavity of length 2L. With a reduction in Δ the halfwidth of the beam at an ordinary mirror is lessened, and at an OVF mirror is increased. Furthermore, with $\Delta \to 0$ the distribution of the mode field of a cavity at the OVF mirror approximates the distribution of the mode field at mirrors of a concentric cavity of length 2L. Thus, by varying the ratios of the cross dimensions of the cavity's mirrors, Δ, it is possible to alter substantially the spatial distribution of fields excited in it. Let us note that ω and ω_0 do not depend on the absolute values of the transverse dimensions of the mirrors and for real dimensions of mirrors a_1 and a_2 are much less than one and $\omega, \omega_0 \ll a_1, a_2$. It is precisely for this reason that the solutions to equation (2) approximate well the behavior of the solutions to equation (1).

Bibliography

1. Zel'dovich, B.Ya., Popovichev, V.I., Ragul'skiy, V.V. and Fayzulov, F.S. PIS'MA V ZHETF, 15, 160 (1972).

2. Hellwarth, R.W. J. OPT. SOC. AMER., 67, 1 (1977).

3. Lesnik, S.A., Soskin, M.S. and Khizhnyak, A.I. "Tezisy dokladov I Vsesoyuznoy konferentsii 'Problemy upravleniya parametrami lazernogo izlucheniya'" [Theses of Papers at the First All-Union Conference "Problems in Controlling Parameters of Laser Emission"], Tashkent, 1978, 119.

4. Bel'dyugin, T.M., Galushkin, M.G. and Zemskov, Ye.M. KVANTOVAYA ELEKTRONIKA, 6, 38 (1979).

5. Vaynshteyn, L.A. "Otkrytyye rezonatory i otkrytyye volnovody" [Open Cavities and Open Waveguides], Moscow, Sovetskoye Radio, 1966.

6. Bel'dyugin, T.M., Zemskov, Ye.M., Mamyan, A.Kh. and Seminogov, V.N. KVANTOVAYA ELEKTRONIKA, 1, 881 (1974).

CSO: 1862
8831

END